Chapter 1 Introduction

1.1 Introduction

In Taiwan, most of the sources of drinking water come from the artificial Reservoirs. For example, Te-Chi Reservoir locates at the upstream of Ta-Chia creek and is used to supply drinking water to Taichung metropolitan. In this study, the water samples were collected from a eutrophicated water body, Te-Chi Reservoir, and treated with XAD resins to separate the natural organic matters (NOMs) into five types. Recently, the quality of the Reservoir water degraded and eutrophication phenomenon became worse due to the soil erosion and overdeveloping deposit. The eutrophicated water generates large amount of disinfection by-products (DBPs) during the chlorination at downstream water intake. The components and properties of organic matters are very complicate on different contaminants, which may cause the serious problems to human health.

Some species of NOMs, e.g. humic acids and related substances, are known to form carcinogenic or mutagenic by-products during chlorine

disinfection. In literature review, XAD resins had been used to isolate and concentrate various NOMs species. Their disinfection by-products formation potentials (DBPFP) were investigated. Among many organic species isolated from natural water, humic acids have been found to be the predominant species to form cancer-causing by-products. These species of NOMs are difficult to quantify, and their presence in water is often measured by their formation of cancer-causing potentials such as trihalomethane formation potential (THMFP) and haloacetic acid formation potential (HAAFP) after chlorination. Specific functional group containing in HAs is related to their THMFP and HAAFP. Hence, detecting the functional groups in NOMs may provide a direct quantitative indication of the characteristics of NOMs in water. Studying the composition and distribution of functional groups in NOMs can be carried out using the Fourier transform infrared spectrum (FTIR) and the ^{13}C nuclear magnetic resonance spectrums (^{13}C-NMR). Only Te-Chi Reservoir raw water and HAs extracted from Te-Chi Reservoir raw water were conducted to the ozone treatment because HAs is the major contributors of disinfection by-products among all the isolated species. Changes of the functional group for the NOMs in water samples before and after the ozonation are investigate using the techniques of ^{13}C-NMR and FTIR.

The advanced oxidation process (AOP) is one of the most effective and latest techniques among many drinking water treatment methods. It utilizes the high oxidation power of free radicals to decompose target substances. Normally, chemical oxidation processes generate free radicals to decompose organic matters in drinking water. While ozone has high oxidation potential (2.07 volts vs. 1.36 volts for chlorination), fast reaction rate, leaving no residues, and easy to retrofit. Ozone has been demonstrated to oxidize a variety of inorganic matters, humic substances and toxicity contaminants found in drinking water. Hence, the ozonation process is preferred in many instances to treating drinking water for achieving both disinfection and oxidation.

The overall ozone oxidation reaction is accomplished in two pathways: direct reaction by ozone molecule and indirect reaction by hydroxyl radicals. The direct ozone oxidation reaction is highly selective but relatively slow by selectively attacking the unsaturated electron-rich bonds contained in specific functional groups, such as aromatics, olefins and amines. In contract, the indirect reaction has a relatively low selectivity but a quick reaction rate by free radicals, which are generated by the decomposition of ozone molecule decomposition. The hydroxyl radicals can oxidize regular

organic substrates, micro organisms or NH_3 to form different strong radicals usually represented as a simplified "·R". The ·R radicals can react with ozone molecule to generate more hydroxyl radicals for further oxidation. However, the formation of free radicals from ozone is affected by either the solution pH or the presence of some scavengers in the water to be treated.

Hydroxyl radicals may react preferentially with CO_3^{2-} and HCO_3^- to produce radicals with weaker oxidation potential, i.e. $\cdot CO_3^{2-}$ and $\cdot HCO_3^-$. The rate constants of inhibition reaction between carbonate, bicarbonate and hydroxyl radicals are 3.9×10^8 and 8.5×10^6 M^{-1} sec^{-1}, respectively (Buxton et al., 1988). Therefore, both CO_3^{2-} and HCO_3^- will behave as scavengers to eliminate the indirect reaction in many AOP under non-acidic conditions. Carbonate and bicarbonate are used in this study to investigate related AOP and investigate the direct and indirect oxidation in ozonation reaction. In the absence of significant quantities of carbonate and bicarbonate, the ozone oxidation reactions proceed in both direct and indirect oxidations. For samples spiked with carbonate and bicarbonate to scavenge hydroxyl radicals, the oxidation is accomplished through only direct reaction. Hence the direct and indirect ozone oxidations can be separately.

In this study, on-line measurement of oxidation reduction potential (ORP), dissolved ozone (DO_3) and pH can be applied to simulate reaction model and system control of AOP. The ozone oxidation reaction is a rapid process; therefore, a fast acquisition of redox reaction information is necessary to conduct the study. The ORP, DO_3 and pH signal measured with the probe, respectively, can be processed with an oscilloscope, which is capable of collecting extremely sensitive data and to the rapid change of electric current. Using a high-frequency signal generator and a GHz digital storage oscilloscope, the signal can be measured in step of 10 ps with good reproducibility. The ORP, DO_3 and pH probes connected to an oscilloscope is capable of collecting 2,500 sets of data within one second so that reliable ORP data can be used for real-time control of the ozonation treatment process.

1.2 Objective

The objectives of this study are as following,

1. Understanding the basic water quality, the composition of NOMs and DBPFP.
2. Applying the on-line oscilloscope for ORP, DO_3 and pH measurements, together with high performance liquid chromatography (HPLC) for measuring the OH radicals in order to investigate the direct and indirect reaction of ozonation mechanism in the presence and absence of quenching inhibition systems.
3. Using the analysis of ORP, DO_3, pH and OH radicals in ozonation to develop an additional Nernst model.
4. Applying FTIR and ^{13}C-NMR to investigate the change of the functional groups after ozonation.

Chapter 2 Literature review

2.1 Natural organic matters in eutrophication reservoir water

The resources of drinking water are very precious, especially for an island such as Taiwan, which strongly depended on the man-made Reservoirs. Te-Chi Reservoir supplies water to metropolitan Taichung area, central Taiwan, ROC. Te-Chi Reservoir suffered from excess agricultural discharge containing chemicals and fertilizers from the upstream and caused serious eutrophication problems. Eutrophication contains substantial amount of organic matters, which may cause serious water quality problems, i.e., taste, odor and color.

NOMs include HAs, hydrophilic acids, proteins, lipids, carbohydrates, amino acids and hydrocarbons (Leenheer, 1981). Humic acids have been strongly implicated as the organic precursor for THMs in drinking water (Rook, 1977). The distributions of NOMs are important information to understand the characteristics of raw water. Isolation of NOMs from raw water by using of resins is a well established procedure. Leenheer (1981) established the procedure to isolate hydrophobic bases, hydrophobic acids,

hydrophobic neutrals and hydrophilic fractions by using XAD-8 resins. Thurman and Malcolm (1981) used XAD-8 resins to isolate HAs and FAs from Suwannee River in southern Georgia, Biscayne groundwater near Miami, FL and the Laramie-Fox Hills groundwater, Superior, CO.

2.2 Application of ozone

There is an increasing interest in utilization of AOP for destruction of recalcitrant compounds. Wang et al. (2004) cited that AOP are characterized by generation of highly reactive radical's intermediates, especially the hydroxyl radicals and have strong oxidation capability to decompose the organic matters or mineralize many synthetic organic chemicals further. Ozone oxidation studies have demonstrated relatively low rate of mineralization so far. However, it was shown that ozonation improved biodegradability of textile baths (Baban et al., 2003). Ozonation is one of the most popular techniques applied in drinking water treatment for disinfection and decomposition of the substances responsible for musty taste and odors in tap water (Utsumi et al. 2003; Peña et al., 2003). Due to its strong oxidation capability and no residual left in water, ozonation step would be the better drinking water treatment (Von Gunten, 2003a, Von Gunten, 2003b).

2.3 Disinfection by-products (DBPs)

During disinfection, the NOMs may produce serious DBPs which contain the halides in organic compounds such as THMs, HAAs and AOX. Humic substances are known to be a source to form THMs during chlorination in water treatment. In USA, a stepwise restriction of DBPs law is enforced to meet future requirements. The maximum allowable contaminant levels of 0.10 mg/L and 0.06 mg/L for total THMs and HAAs were restricted by the National Primary Drinking Water Regulation. The National Secondary Drinking Water Regulation is more restricted to decrease the maximum contaminant levels to 0.040 mg/L and 0.030 mg/L for THMs and HAAs, respectively. Ho et al., (2002) cited that ozone is commonly used in water treatment for disinfection and for the oxidation of organic compounds. It can react rapidly with the NOMs present in waters. The ozonation of NOMs in water is still not well understood because NOMs consists of a diverse range of compounds with very different chemical properties. Since the removal of NOMs is important in water treatment (in order to improve the water quality) then there is a need to better understand the effect different NOMs characteristics have on the decomposition of ozone.

2.4 Two stage ozone reaction

Ozone has higher oxidation potential (2.07 volts) than Cl_2 (1.36 volts). Hence, ozonation can be used to purify drinking water for both functions of disinfection and oxidation (Rice et al., 1981). The concentration of ozone molecule is influenced strongly by pH levels. Alaton et al. (2002) found a fast decay rate of dye contributed by free radicals oxidation at high pH levels. This is due to the hydroxide ions enhance the self-decomposition of ozone to generate hydroxyl radicals in basic condition. The oxidation potential of hydroxyl radicals is much higher than that of molecular ozone. On the other hand, a lower formation rate of hydroxyl radicals obtained in acidic condition during treatment of wastewater containing 2,4-dichlorophoxyacetic acid (Chu and Ching, 2003). The hydroxyl radicals' formation rate decreased by a factor of 10 for decreased a pH level (Staehelin and Hoigne, 1985). Therefore, at high pH condition, indirect hydroxyl radicals reaction predominates the ozonation reaction (Chu and Ching, 2003). The process of ozone oxidation in water can be classified into two pathways: ozone molecular direct reaction and hydroxyl radicals' indirect reaction (Hoigné and Bader, 1976).

1. Ozone molecular direct oxidation:

   Ozone selectively attacks the unsaturated electron-rich bonds

and easily reacts with specific functional groups, such as aromatics, olefins and amines (Hoigné and Bader, 1983). In general, the reaction by direct ozone reaction is slower than that of hydroxyl radicals' reaction.

2. Hydroxyl radicals indirect oxidation:

The indirect reaction of hydroxyl radicals is generated by the ozone molecule decomposition, while the hydroxyl radicals' reaction rate is fast and the selectivity is low (Prado et al., 1994). In water, ozone may react directly with dissolved substances, or it may decompose to form secondary oxidants. Among these secondary oxidants, hydroxyl radicals are extremely powerful and non-specific oxidants that react with many organic and some inorganic species (Pi et al., 2005). In pure water, decomposition of the ozone becomes accelerated by increasing the pH (Staehelin and Hoigné, 1982). In aqueous solutions, the decomposition of ozone at a given pH is often accelerated by a radical type chain reaction which can be initiated, promoted, or inhibited by various solutes (Staehelin and Hoigné, 1985). Staehelin and Hoigné observed that organic solutes which can convert hydroxyl radicals into $\cdot O_2$ (superoxide radical ions) always accelerate the decomposition of ozone unless an ample amount of radicals scavengers is present. However, its short lifetime (10^{-9} s) hinders its direct detection

(Louit et al., 2005).

2.5 Scavenger and hydroxyl radical measurement in ozonation

The well-known radical scavengers, carbonate and bicarbonate, were be used in several studies to investigate related AOP (Staehelin and Hoigné, 1985; Ma and Graham, 2000; Chu and Ma, 2000; Alaton et al., 2002). The rate constants of inhibition reaction between carbonate, bicarbonate and hydroxyl radicals are 3.9×10^{8} and 8.5×10^{6} M^{-1} sec^{-1} (Buxton et al., 1988). That is the formed hydroxyl radicals in reactor may react with carbonate and bicarbonate immediately. Therefore, the carbonate and bicarbonate can serve as a scavenger for hydroxyl radicals. Thus, the carbonate and bicarbonate ions are widely applied as hydroxyl radicals' scavengers to study the direct and indirect oxidation in ozonation reaction (Chu and Ma, 2000).

Ho et al., (2002) cited that ozone reaction is known to produce secondary oxidants such as the hydroxyl radicals, a much more powerful oxidant than ozone. This can be beneficial as hydroxyl radicals can react non-selectively to oxidize a broad range of organic compounds. Utsumi et al. (2003) also reported that hydroxyl radicals are one of the most reactive species in ozonation of water and the amount of hydroxyl radicals seems to

determine the efficiency of ozonation. However, there have been very few papers which determined the amount and the dynamics of hydroxyl radicals directly. Therefore, the measurement of hydroxyl radicals was important for investigating the ozonation mechanism. Utsumi et al (2003) also cited that hydroxyl radicals are proposed as an important factor in the ozonation of water. It was difficult to measure hydroxyl radicals because the hydroxyl radicals are unstable. Zuo (2003) cited that due to the high reactivity of hydroxyl radicals with organic, the concentrations of hydroxyl radicals are extremely low and very difficult to quantify. Recently, several investigators have used a free radicals quenching technique to determine the photo-chemical production rates of hydroxyl radicals in natural waters. In order to detect free radicals, HPLC is widely utilized because of its sensitivity and selectivity, and HPLC technique has been developed to detect unstable radicals. Since HPLC analysis used the steady-state measurements, thus allowing identification of the products of coumarin under various conditions; wherever possible these products have been quantified (Louit et al., 2005). This study has succeeded in direct determination of hydroxyl radicals' generation in water during ozonation by HPLC technique.

2.6 Application of on-line oscilloscope to monitor the ozonation

Ozonation is a rapid process; therefore, the fast acquisition of redox reaction information is required. Oscilloscope has the advantages such as a rapid collection of experimental data which were converted by voltage peaks and pulses in the instantaneous change. It has extremely sensitiveness and fast collection speed that can precisely obtain experimental data. Saito and Hyodo (2003) using BaF_2 and plastic (BC-422) scintillates to measure the time resolutions of a new positron lifetime spectrometer based on a fast digital oscilloscope. Landgraf (2001) applied in time-resolved detection of crude oil as an example for investigation the possible practical applications. Signals can be measured in step of 10 ps with good reproducibility using a high-frequency signal generator and a GHz digital storage oscilloscope. This study attempted to understand the ozone mechanism by connecting a digital oscilloscope.

Nicoli et al. (2004) cited that ORP measurements are suitable to evaluate the ability of reducing compounds to promote electron transfer. On the other hand, the mentioned kinetic methods allow us to measure the chain-breaking activity of both electron-transferring and hydrogen-donating antioxidants. The oxidation/reduction state of a chemical reaction system

can be indicated by its ORP value. On-line ORP measurement can be easily carried out using an ORP probe. In addition, the pH and DO_3 were also connected with oscilloscope for investigating the ozonation mechanism.

2.7 Change of functional groups during ozonation

The compositions of NOMs functional groups can be determined by Fourier transform spectrophotometer (FTIR) and CPMAS Carbon 13 nuclear magnetic resonance spectrums (^{13}C-NMR) (Leenheer et al., 2003a; Leenheer et al., 2003b). Calace et al. (1999) applied FTIR to study the distribution of functional groups on HAs and FAs from Martignano Lake (Japan). The FTIR spectrum showed that the natural HAs contain the functional group mainly unsaturated bonds of aromatic, C=O of carboxylic acids and O-H of phenol. From FTIR analysis, Ma and Chu (2001) found the aliphatic functional groups were the apparent majority on HAs and FAs from water. The proportion of isolated component of aliphatic was HAs < FAs < hydrophilic fractions, while the aromatic was hydrophilic fractions < HAs < FAs, respectively.

Carbon thirteen nuclear magnetic resonance is a very useful tool in determining the average chemical structure of NOMs. Spectrum can be

obtained from a concentrated liquid or a solid sample and the chemical shifts of the spectral peaks are assigned to ^{13}C in different chemical environments. The areas under the peaks are related to the percentages of different carbon in each of the chemical environments (Newcombe et al., 1996). Leenheer et al. (2003a) used the ^{13}C-NMR to investigate the functional groups of isolated natural hydrophobic organic acids from Anaheim Lake and Colorado River of USA. Pomes et al. (2000) used the XAD-8 resins to isolate HAs and FAs from the Wakarusa River in USA for ^{13}C-NMR analysis. González-Vila et al. (2001) also characterize aquatic FAs and HAs using ^{13}C-NMR spectroscopy. These studies showed the mainly content of carbon are aromatic carbons for HAs. According to proposed structures, the aromatic carbon content on FAs is less than that of HAs. The aliphatic carbon content was much more than that of aromatic on FAs.

Chapter 3 Materials and methods

3.1 Experimental design

The sampling site in this study is located at Te-Chi Reservoir, which was subject to the discharge of chemicals and fertilizers from the agricultural activity for a long time. The applied ozonation study samples were from raw water of Te-Chi Reservoir raw water and HA extracted form Te-Chi Reservoir raw water. In order to understand the two step ozonation (O_3 and hydroxyl radicals' reaction), the effect of scavenger addition on the inhibition of indirect free radicals reaction was applied. Then the on-line oscilloscope monitor could help to investigate the fast chemical redox reactions. Measured hydroxyl radicals provided the direct data to find out the ozonation. Therefore, the process via either direct or indirect ozone oxidation could be investigated individually.

Experimental flow chart is shown in Figure 3.1 and the detailed steps are described as follows.

(1) Sample preparation and analysis: Collect water sample from Te-Chi Reservoir and analyze some basic water qualities (pH, DO, TDS, temperature and conductivity) on site. After the water sample was

filtered with a 0.45μm filter membrane in the laboratory, the following basic water analysis was conducted. The items analyzed were COD, DOC, hardness, alkalinity, and NH_3-N.

(2) Isolation and fractionation: The extraction procedures utilized in this study followed the procedures described by Thurman and Malcolm (1981) and Leenheer (1981). This method using Amberlite XAD-8 (Amberlite XAD, Sigma, USA), which was packed in Pyrex glass columns to isolate the five categories of organic fractions such as HAs, FAs, hydrophobic neutrals, hydrophobic bases and hydrophilic fractions. In order to investigate the disinfection by-products formation potential (DBPFP) of the separated five species of organic matters, dose chlorine to analyzes DBPFP.

(3) Ozone and quenching test: Te-Chi Reservoir raw water and HAs extracted from Te-Chi Reservoir raw water were used as the precursor to carry out the non-inhibit and inhibit quenching ozonation tests, which was monitored by on-line oscilloscope system. The data of ORP, pH, DO_3 and A_{254} which were on-line monitored, were used to investigate the two step ozonation. The DBPFP was measured by dosing sufficient chlorine to the samples. The samples are collected and freeze-dried before they were analyzed by the ^{13}C-NMR and FTIR.

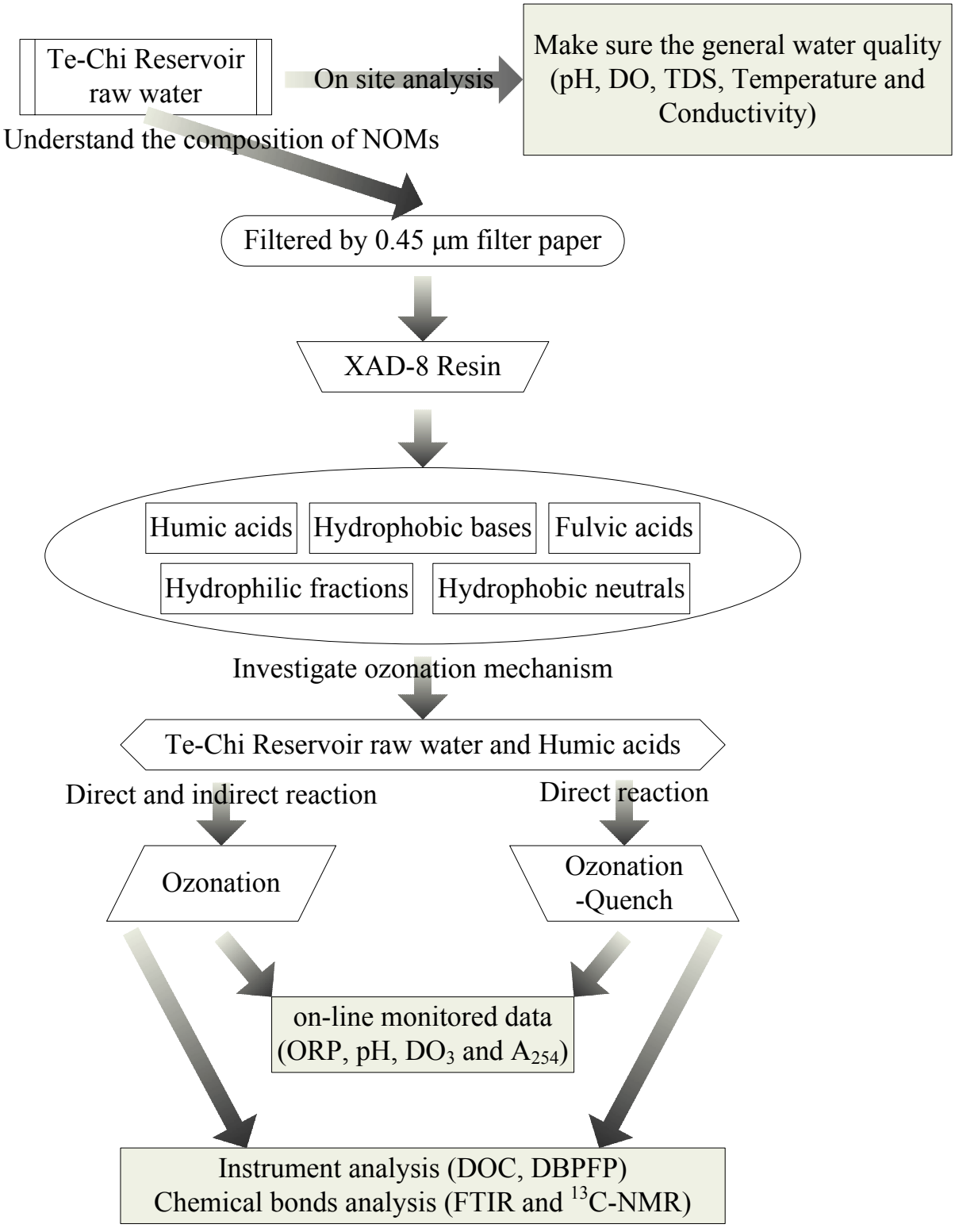

Figure 3.1 The experimental design for ozonation and analysis in this study.

3.2 Methods and Instruments

3.2.1 Sampling site

The sampling time was on September 30, 2004 and 20 L of Te-Chi Reservoir water were filled in polyethylene buckets. They were sealed up and covered with black plastic bags to prevent reaction with sunlight. The water sample was refrigerated at 4ºC before amalysis. The items analyzed in field were pH, DO, total dissolved solids (TDS), water temperature, and conductivity. The sampling location is shown in Figure 3.2.

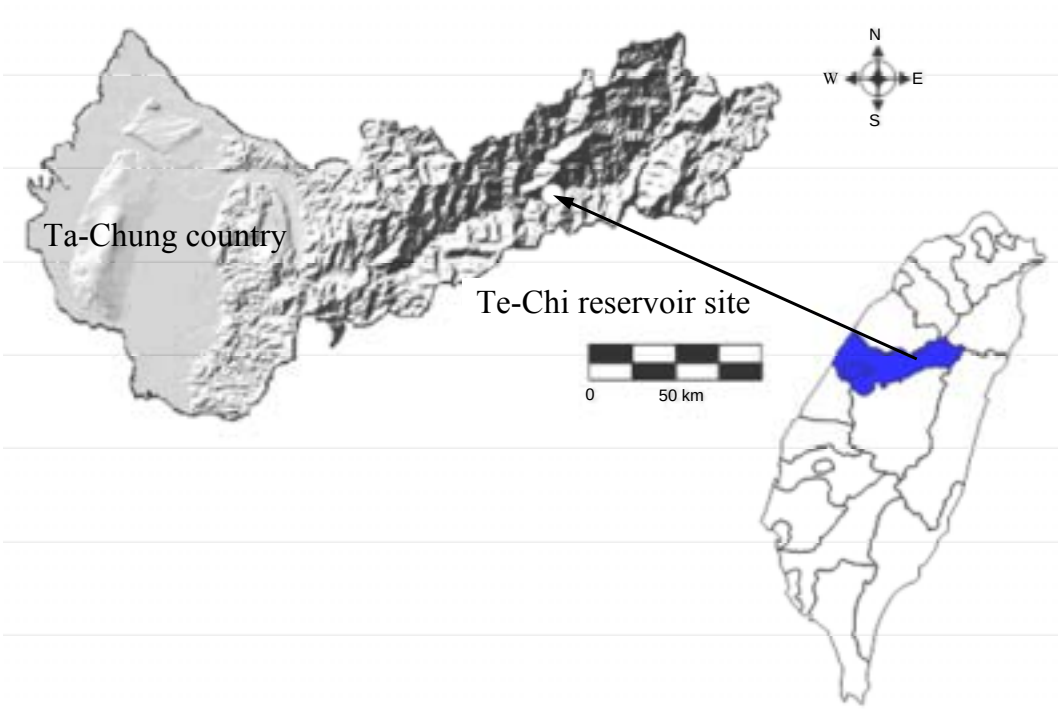

Figure 3.2 Sampling location of Te-Chi Reservoir, which provides water for domestic water in Tai-Chung area, central Taiwan, ROC.

3.2.2 Isolation and fraction

Pre-treatment of XAD-8 resins

(1) Cleaned the resins, and then immerged in a 0.1 N NaOH solution for 72 h, followed by a washing step with pure water.

(2) Resins were then placed in a Soxhlet extractor and washed with methanol, hexane, acetonitrile and methanol, respectively, for 24 h.

(3) After this, the resins were rinsed with pure water several times to remove the residual methanol; the resins were then packed in Pyrex glass columns (5 cm internal diameter (ID) and 60 cm in length).

(4) Passing 1 L of 0.1 N NaOH and 1 L of 0.1 N HCl (flow rate: 25 mL/min) through the resins in the glass chromatographic analysis tube, and repeated twice. To make sure no methanol was left in XAD-8 resins, the effluent of the rinsed water was examined by TOC analysis. The procedures of cleaning the resins with pure water are repeated until the TOC concentration in the effluent was below the detection limit of 0.02 mg/L.

The isolation procedures utilized in this study have been described by Thurman and Malcolm (1981) and Leenheer (1981), which obtained five types of NOMs: hydrophobic bases, hydrophobic acids (include: HAs and

FAs), hydrophobic neutrals, and hydrophilic fractions. Amberlite XAD-8 (Amberlite XAD, Sigma, USA) was used as an absorbent for the separation. The regents and equipments for resins separation process were shown in Table 3.1. The procedures for separation of five species of NOMs from Te-Chi Reservoir raw water were described in Figure 3.3. At first, the 100 L raw water sample was filtered by passing through a 0.45 μm cellulose acetate filter membrane to remove the suspended solids, and then the pH value was adjusted to 7 by adding HCl. After that, the filtered water was passed through the first XAD-8 resin column at a flow rate of 25 mL/min followed by eluting with 0.1 N HCl to recover the hydrophobic bases, which was adsorbed on the resins. The pH of the effluent from the first XAD-8 column was adjusted to 2 with 2 N HCl. The brown solution was then introduced into a second XAD-8 resin column at the same flow rate of 25 mL/min. The NOMs contained in the filtrate from the second XAD-8 column was collected as the hydrophilic fractions. A brown solution was obtained by eluting the NOMs absorbed on the second XAD-8 resins with 0.1 N NaOH. The pH of this brown solution was adjusted to 1 with 0.1 N HCl. It was then passed through a 0.45 μm membrane filter. The filtrate contained FAs and HAs residues were left on the membrane filter. The HAs particles were removed from the membrane filter by dissolving in 0.1 N

NaOH and preserved in polyethylene bottles. The remaining XAD-8 resins left in the second column was removed, dried at 60ºC and washed with methanol to collect hydrophobic neutrals. A vacuum instrument combined with high-purity nitrogen gas (99.99%) was used to evaporate the methanol solution. The concentrated hydrophobic neutrals were dissolved in pure water as a stock solution.

Table 3.1 Summaries of the regents and equipments for nature organic matters water separation by resin extraction process.

Equipment	**Series Number, Maker, Country**
XAD-8 resins	Amberlite XAD-8, Sigma, USA
Glass column	Pyrex 5cm, ID×60 cm, local supply
Teflon tubing	Reorder#06409-14, USA
Peristalsis pump	Peristaltic pump System Model No. 7553-80, Cole-Parmer, USA
Soxhlet extractions	Pyrex, local supply
Reagent (GR)	**Catalog Number, Maker, Country**
NaOH	R.D.H., R30620, Germany
Methanol	Merck, 6009, Germany
Hexane	Merck, 4367, Germany
Acetonitrile	Merck, 3, Germany`

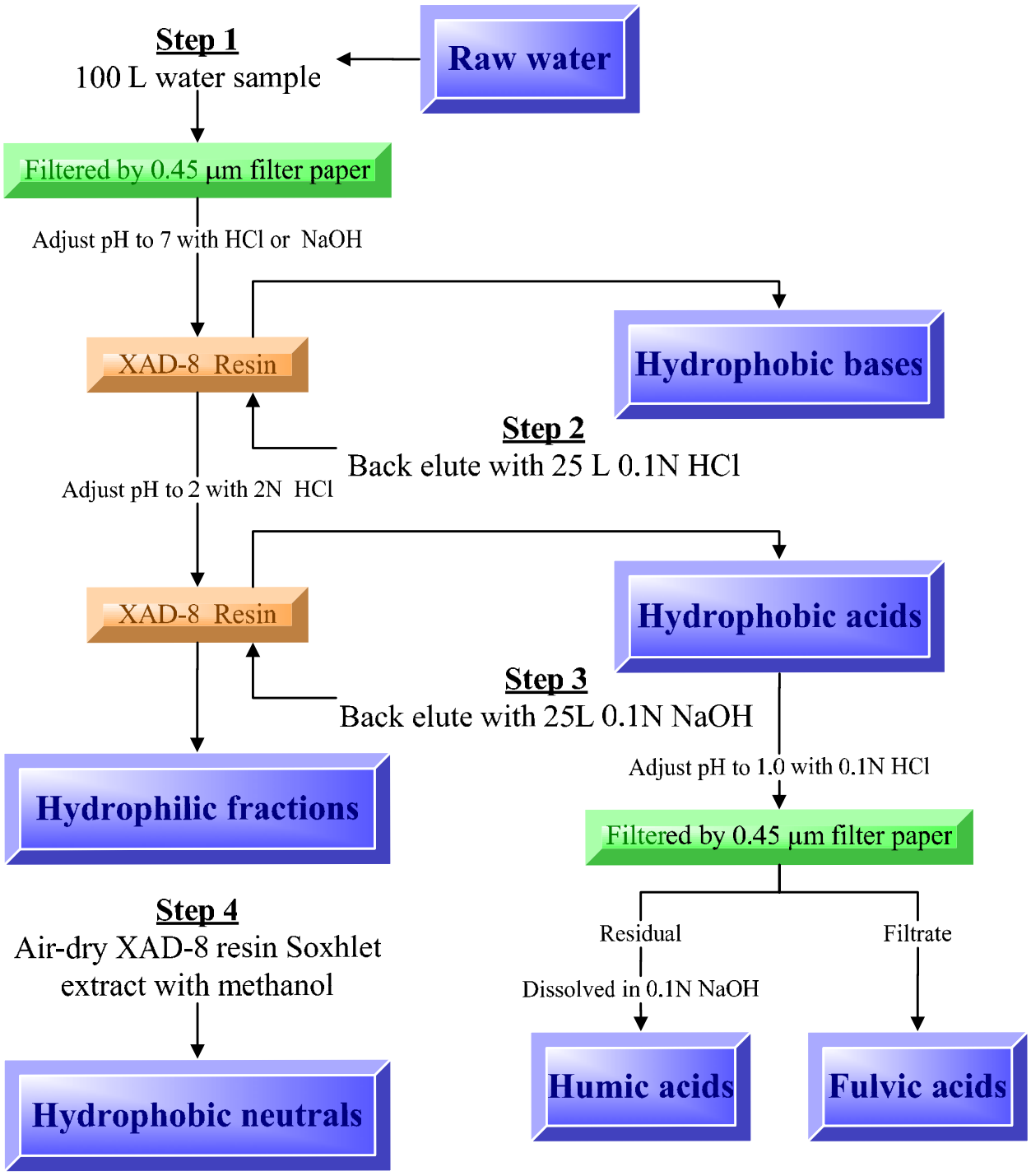

Figure 3.3 The flowchart of five species of NOMs (HAs, FAs, hydrophobic neutrals, hydrophobic base and hydrophilic fractions) extracted from Te-Chi Reservoir raw water by resins separation process.

3.2.3 Disinfection by-products Formation Potential (DBPFP) Studies

The DBPFP used hypochlorite (OCl^-) on Te-Chi Reservoir raw water and five species of NOMs extracted from Te-Chi Reservoir raw water which conducted in 40 mL closed Pyrex glass vials. The initial ratio of OCl^-/DOC for each sample was adjusted to 3. KH_2PO_4 and NaOH were used to prepare a buffer solution in order to maintain the constant pH before chlorination. Chlorination of the water sample was incubated at 20ºC for 7 days. After incubation, $Na_2S_2O_3$ was added to remove residual chlorine and prevent additional chemical reactions between OCl^- and DOC.

3.2.4 Ozonation system

A schematic diagram of the ozonation apparatus is shown in Figure 3.4. 5 L batch Pyrex glass reactor equipped with a 275 rpm mixer and three monitored sensors (pH, ORP and DO_3) connected with oscillographic recorder were used in this study. Oscillographic recorder (Yokogawa, OR100E, Japan) connected with pH, ORP and DO_3 sensors can be utilized to monitor and record instantaneous redox potential, pH profiles and the change of DO_3 during ozonation. UV detector connected with the probe of optical fiber for monitoring the change of absorbance at 254 nm in ozonation system. The reaction temperature was maintained at 25±2ºC by

submerging in a constant temperature water bath outfitted with a temperature controller. Each set of semi-batch test was carried out by introducing ozone into the batch reactor. A laboratory scale ozone generator (KA-1600, AirSep Corp., USA) was used to generate 10.53 g/h of ozone in the reactor. The maximum practical ozone concentration in pure water was found to be 2.8 mg/L.

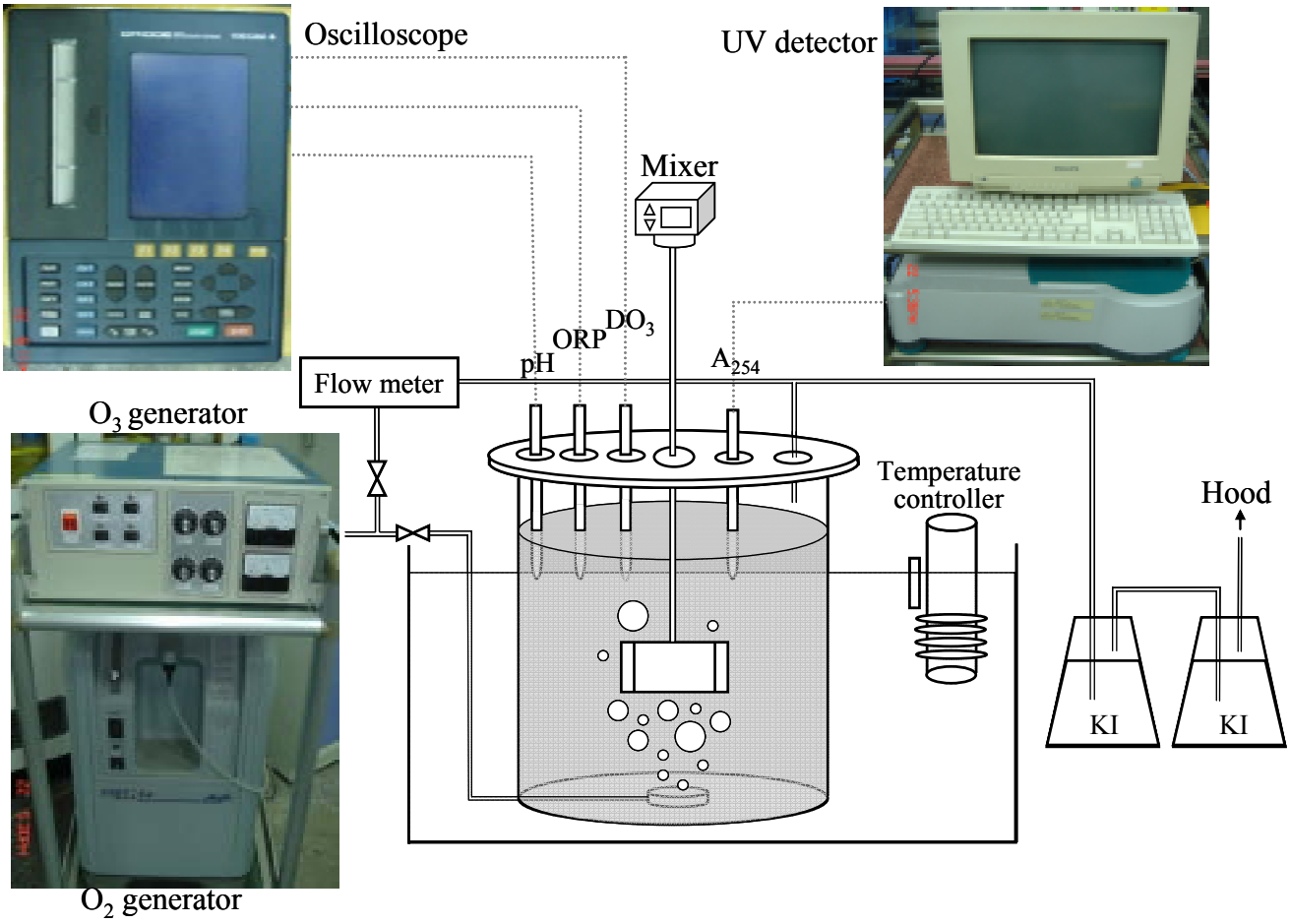

Figure 3.4 Schematic of diagrams ozonation apparatus.

3.2.5 On-line oscilloscope monitor apparatus

The oscillographic recorder (Yokogawa, OR100E, Japan) connected with pH, ORP and DO_3 sensors. It can directly collect huge of data during ozonation at the same time. Without personal computer, the oscillographic recorder can record data by its own file type, then transfer to excel file type. The comprehensive data collection system can store 16,000 data per second and is useful to understand the rapid ozone direct and indirect reactions.

3.3 Analysis Methods

3.3.1 Basic water quality analysis

Basic water analysis is referred to Standard Methods 20th Ed., (APHA et al., 1998). The names of the corresponding methods are listed in Table 3.2.

Table 3.2 Basic water quality analytical items and methods.

Items	**Standard method***
pH	pH meter, Suntex, TS-1 (4500-H^+ B)
Temperature	Thermometer mothod (NIEA W217.50A)
DO	DO meter, WTW, Microprocessor, Oximeter (4500G)
TDS	Conductivity Meter, WTW, LF 95
COD	Titrimetric Method (5220C)
Specific conductivity	Conductivity Meter, WTW, LF 95 (2510B)
Hardness	EDTA Titration Method (2340C)
Alkalinity	Titration Method (12320B)
NH_3-N	Titrimetric Method (4500-NH_3)

*Standard methods for the examination of water and wastewater 20th edition. (APHA et al., 1998)

3.3.2 Trihalomethanes (THMs)

Analysis of THMs is referred to Standrad Methods 20th Ed., 6232D (APHA et al., 1998). A 1 mL sample is pretreated by using a Purge & Trap instrument (Tekmar LSC 2000, Cincinnati, Ohio, USA) and then automatically injected into a gas chromatography equipped with an electron capture detector (GC/ECD) (GC-14B, Shimadzu Co., Kyoto, Japan) connected to a recorder (SIC Chromatocorder 12, Alphatech Corp., Tokyo, Japan). The summary of the calibration equations for THMs are listed in Table 3.3. The MDL range was between 1.5 and 2.3 μg/L. Table 3.4 is the summary of the reagents and equipments used for THMs analysis. The purge and trap and GC/ECD analysis conditions of THMs are shown in Table 3.5.

Table 3.3 Summaries of the calibration equations for THMs.

Species	Calibration Equation	Range (μg/L)	R^2	MDL** (μg/L)	Recovery*** (%)
TCM	Y* = 1,984x + 2,376	5-500	0.996	2.3	96.2 ± 3.2
DCBM	Y* = 8,624x + 8,512	5-500	0.995	1.8	97.1 ± 2.3
DBCM	Y* = 665,648x + 9,898	5-500	0.993	1.5	96.3 ± 2.1
TBM	Y* = 422,732x + 8,027	5-500	0.996	2.1	96.5 ± 2.8

*peak area

** MDL: Select a concentration which is slightly higher than the lowest concentration in calibration curve and make 7 replicate analysis. 3-times standard deviation (the data of 7 replicate analysis) in terms of concentration unit is the MDL value.

***Recovery: Sample concentration is (a) Adding standard known concentration sample (b) into the sample and obtain the final concentration (c) The recovery (%) is expressed as [(c-a)/b]×100. Mean and std. dev. of triplicates.

Table 3.4 Summaries of the reagents and equipment used for THMs analysis.

Reagent	**Series Number, Maker, Country**
THMs Standards (10^2 ppm)	Standard # C-188-01, NSI Environmental Solutions, USA.
NaOCl	R13440, R. D. H., Germany
NaOH	R30620, R. D. H., Germany
KH_2PO_4	R30407, R. D. H., Germany
$Na_2S_2O_3$	R13481, R. D. H., Germany
Equipment	**Series Number, Maker, Country**
Gas chromatograph Electron-Capture Detector	GC-14B, Shimadzu Co., Kyoto, Japan
Recorder	SIC Chromatocorder 12, Alphatech Corp., Tokyo, Japan.
Purge and Trap	Tekmar LSC 2000, Cincinnati, USA
40 mL brown bottle	

Table 3.5 Purge & trap and GC/ECD analysis conditions of THMs.

Purge and Trap	**Operation Conditions**
Purge Gas	N_2 (g) (99.999 %), Flow rate = 40 mL/min
Purge Time	11 min
Cap Cool Down Temp	-150ºC
Desorb Preheat Temp	175ºC
Desorb	4 min at 180ºC
Inject	1 min at 180ºC
Bake	10 min at 225ºC
GC	**Operation Conditions**
Column	Fused silica, SGE BP5, 50 m × 0.22 mm i.d., 1.0 μm film, high polarity
Program	50ºC, 3 min→5ºC /min→200ºC, 5 min
Carrier Gas	N_2 (g), head pressure = 0.8 kg/cm^2, Flow rate =10 mL/min
Injection Temp.	200ºC
Detector Temp.	260ºC
ECD	**Operation Conditions**
Range	10
Current (nA)	1

3.3.3 Haloacetic acids (HAAs)

The analytical procedure for HAAs is followed Standard Method 20th Ed., 6233B (APHA et al., 1998). Prior to analyzing the HAAs, the water sample was acidified and extracted with methyltertbutylether (MTBE), then add diazomethane to from methyl ester derivative. The extracted sample was injected into the GC/ECD (China Chromatograph 9800, Taipei, Taiwan, ROC.) for analyses of HAAs. The summary of the calibration equations for HAAs are shown in Table 3.6. The range of recovery was between 95.6 and 98.8%. Table 3.7 is the summary of the reagents and equipments used for HAAs analysis. The purge and trap and GC/ECD analysis conditions of HAAs are listed in Table 3.8.

Table 3.6 Summaries the calibration equations for HAAs.

Species	Calibration Equation	Range(μg/L)	R^2	MDL**(μg/L)	Recovery***(%)
MCAA	Y* = 2,314x + 26,575	5-500	0.994	1.7	96.5 ± 2.2
DCAA	Y* = 1,526x + 34,392	5-500	0.996	1.3	95.6 ± 2.3
TCAA	Y* = 1,880x + 84,370	5-500	0.995	1.4	96.6 ± 1.8
MBAA	Y* = 2,154x + 91,386	5-500	0.993	1.2	96.2 ± 3.2
DBAA	Y* = 4,542x + 124,706	5-500	0.995	1.3	98.8 ± 2.1
BCAA	Y* = 6,599x + 84,183	5-500	0.995	1.8	97.2 ± 3.1

*peak area

** MDL: Choice a concentration is slightly higher than the lowest concentration in calibration curve and duplicate to analyze 7 times. 3-fold of standard deviation (the data of 7 times analysis) converse into concentration is MDL value.

***Recovery: Sample concentration is a. Adding standard sample (known concentration is b) into sample concentration is a. this mixture concentration is c. finally, calculating [(c-a)/b]*100 and duplicate 3 times to obtain recovery.

Table 3.7 GC/ECD analysis conditions for HAAs.

Item	**Specification and Operation Conditions**
Column	Fused silica capillary (DB-210, J & W, Scientific U.S.A), 30 m × 0.32 mm i.d., 0.5 μm film, high polarity
Program	45ºC, 10 mins → 7ºC /min → 200ºC, 5 mins
Carrier Gas	N_2, 99.999%, flow rate = 1.1 mL/min
Make up Gas	N_2, 99.999%, flow rate = 26 mL/min
Injection Temp.	210ºC
Detector Temp.	260ºC

Table 3.8 Summaries of the regents and equipment used for HAAs analysis.

Reagent	**Series Number, Maker, Country**
MCAA	F2082, Chem. Service, USA
DCAA	F3083, Chem. Service, USA
TCAA	F2084, Chem. Service, USA
MBAA	F2085, Chem. Service, USA
DBAA	F2033, Chem. Service, USA
BCAA	F2031, Chem. Service, USA
HAAs Methylated Mixture	PHM-552M, Ultra Scientific, USA
MTBE	Lot # 856140, Fisher, USA
Na_2SO_4	R37481, R. D. H., Germany
$CuSO_4$	R31293, R. D. H., Germany
KOH	R30603, R. D. H., Germany
Diazald(N-methyl-N-nitroso-p-toluene Sulphonamide)	Lot # 63H3742, Sigma, Germany
Silica gel	R13711, R. D. H., Germany
NH_4Cl	R31107, R. D. H., Germany
Ether	R24005, R. D. H., Germany
Diethylenglykolmonoethylether	R62427, R. D. H., Germany
Equipment	**Series Number, Maker, Country**
Gas chromatograph Electron-Capture Detector, ECD	China Chromatograph 9800, Taipei, Taiwan, ROC.
Recorder	SIC Chromatocorder 12, Alphatech Corp., Tokyo, Japan
Vortex mixer	Scientific Industries, INC., USA

The processes for HAAs analysis are:

(1) To a sample (30 mL) sulfuric acid (20 mL) was added to acidify the solution to the pH value smaller then 0.5.

(2) To the above solution $CuSO_4 \cdot 5H_2O$ (3 g) and Anhydrous Na_2SO_4 (12 g) was added followed by vibrating to dissolve completely by Vortex mixer.

(3) MTBE (3 mL) was added to the sample for extraction by means of vibration extract for 10 minutes.

(4) Supernatant liquid (1.7 mL) was removed into a 2 mL vessel, with adding of diazomethane (0.3 mL) for esterification, and then settle 15 min.

(5) After adding enough silica gel to remove excessive diazomethane and again settles 15 min, 1 μL sample was analyzed by using of GC/ECD.

The installation of diazomethane preparation is show in Figure 3-5:

(1) KOH (37%(w/v), 30 mL) and Diazald solution (4 g Diazald + 20 mL ether + 20 mL Diethylenglykolmonoethylether) was added into wash bottle B.

(2) Enough ether was added into wash bottle A to over the height of diffuser dome.

(3) A steam of nitrogen gas was passed through wash bottle A and then wash bottle B, finally pass approximately 10 mL MTBE on ice bath. Diazomethane would be absorbed by MTBE.

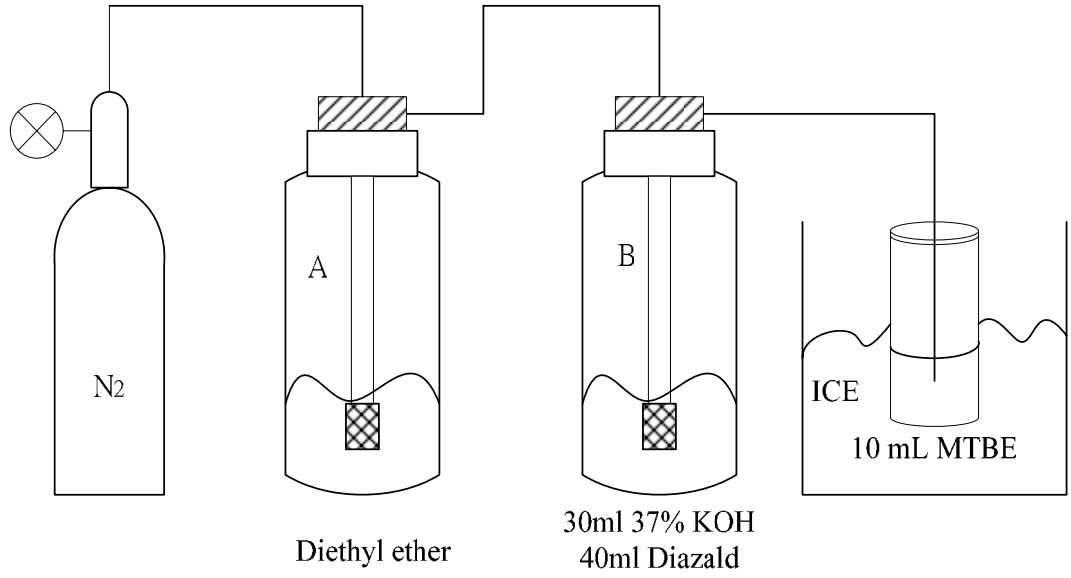

Figure 3.5 Schematic of diazomethane preparation. A stream of nitrogen was purge to wash bottle A and then inducted to wash bottle B, finally pass through approximately 10 mL MTBE on ice bath.

3.3.4 Adsorbed organic halides (AOX)

Analytical procedures for AOX are referred to the Standard Method 20th Ed., Adsorption-Pyrolysis-Titrimetric Method (APHA et al., 1998). Filling the activated carbon to the glass tube column (0.3 cm ID × 2 cm) and 40 mL (5 mL/min) of sample were injected to let the organic and inorganic halides adsorb on the activated carbon. Then, through the injection of 40 mL (5 mL/min) 0.08 M KNO_3 into the activated carbon, replace the inorganic halides. The activated carbon was load onto a quartz sample boat and put it in a high temperature oven (850-900ºC). The organic halides which were adsorbed on the activated carbon would react with oxygen in burning reaction. The products (hydrogen halides) would react with silver electrode and silver ions, instead of halides ions would be measured. Finally, the quantity of halogens would be indicated after conversion to standard unit (chlorine ion values). Table 3.9 was the summary of the reagents and equipment for AOX test. The recovery test of AOX is shown in Table 3.10.

Table 3.9 Summaries of the reagents and equipment for AOX analysis.

Reagents	**Series Number, Maker, Country**
Sodium acetate	6267.1000, Merck, Germany
Glacial acetic acid	200-580-7, R.D.H., Germany
Potassium nitrate	5079.0100, Merck, Germany
2, 4, 6-trichlorophenol	R 22-36/38, R.D.H., Germany
Sodium sulfite	6657. 1000, Merck, Germany
Granular activated carbon	TX070, Mitsubishi Kasei, Japan.
Equipment	**Series Number, Maker, Country**
TOX-10Σ	Mitsubishi, Japan.

Table 3.10 The recovery test of AOX.

Conc. introduced ($\mu g\ Cl^-/L$)[b]	**Conc. found ($\mu g\ Cl^-/L$)[c-a]**	**Recovery (%)**	**Average recovery (%)**
	99.4	99.4	
	101.5	101.5	
100	104.8	104.8	100.5 ± 3.4
	95.6	95.6	
	101.2	101.2	

*Stock solution：0.37 g 2, 4, 6-trichlorophenol in 1 L reagent water (10^3 μg/L of Cl)

*Recovery: Sample concentration is a. Adding standard sample (known concentration is b) into sample concentration is a. this mixture concentration is c. finally, calculating [(c-a)/b]*100 and duplicate 5 times to obtain recovery.

3.3.5 Absorbance at wavelength of 254 nm

During ozoantion, many data (absorbance at 254nm (A_{254})) were collected by UV spectrophotometer (Cary 50, Varian Austrslis Pty Ltd). The probe of optical fiber connects with UV detector and inserts into the reactor for monitoring the twinkling change data. The Cary 50 is powered by the personal computer to control the instrument, and Cary Win UV software was used to set the monitoring condition.

3.3.6 Dissolve organic carbon (DOC)

The procedure for determining the dissolve organic carbon (DOC) is followed to Standard Methods 20th Ed., 5310D (APHA et al., 1998). Concentrations of were DOC determined by a TOC analyzer (Analytical model 1010, OI Co., USA). It applies wet-oxidation method and is suitable to analyze the dissolved organic matter containing water sample. The organic matter of the sample passed through the 0.45μm membrane during filtration is defined as the DOC. The water sample is acidified by adding H_3PO_4 followed by bubbling with N_2 gas to expel the inorganic carbon and volatile organic carbons. The oxidant (sodium persulfate, $Na_2S_2O_8$) is added to the digester and the temperature of mixture is raised to 100ºC. At this point, the organic carbon is converted to CO_2, which was pased through a dried oven and then was measured by NDIR (nondispersive infrared spectrometery) to obtain the DOC concentration. The regents and equipment for DOC analysis are summarized in Table 3.11. The calibration data of DOC analysis are shown in Table 3.12.

Table 3.11 Summaries of the reagents and equipment for DOC test.

Reagent	**Series Number, Maker, Country**
$Na_2S_2O_8$	R31437, R. D. H., Germany
H_3PO_4	R13440, R. D. H., Germany
KHP	R33325, R. D. H., Germany
Equipment	**Series Number, Maker, Country**
TOC	O.I. Analytical Model 1010

* Stock solution：2.128 g KHP in 1 L reagent water (1,000 mg-C /L)

Table 3.12 Summaries of the calibration equation for DOC.

Conc. (mg/L)	Volume (mL)	Peak Area	MDL** (mg/L)
0	20	6,503*	
0.5	20	14,170*	
1.0	20	23,554*	
2.0	20	37,203*	
5.0	20	86,845*	0.01
Calibration Curve			R^2
y = 1603x + 6412			0.999

*n = 3

** MDL: Select a concentration which is slightly higher than the lowest concentration in calibration curve and make 7 replicate analysis. 3-times standard deviation (the data of 7 replicate analysis) in terms of concentration unit is the MDL value.

3.3.7 Hydroxyl radicals determination

Coumarin and 7-hydroxycoumarin at the highest possible grade were obtained from Aldrich chemicals. The HPLC systems with reverse phase chromatographic analysis were 851-AS type auto sampler; UV-970 type detector and PU-980 type pump (Jasco Co.). The chromatographic data system software was used to control the system. The column was a Pharmacia C2-C18 μRPC column ST 4.6/100. The column volume was 1.66 mL. For all analysis, the flow rate was 0.5 mL/min and a gradient elution with two solutions (A and B) was used. Solution A was 89% pure water, 10% methanol and 1% acetic acid, whereas solution B was 89% methanol, 10% pure water and 1% acetic acid. At first, different gradient elution was tested in order to achieve the best possible separation. The following program was chosen: 100% A during 7 minutes, then linear gradient to 70% A and 30% B in one minute and keep at this ratio for 7 minutes, followed by linear gradient to 50% A and 50% B in one minute and keep at this ratio for 9 minutes. In all cases, at least 1000 μL of solution was introduced in a 300 μL injection loop, to ensure a better quantification of the products. The absorbance was measured at wavelength 275 nm, which was chosen in order to obtain sensitive detection towards coumarin irradiation products. Because the standard sample is difficult to obtain; the

calibration equation of 7OH-coumarin was used as the other isomers' calibration equation. The calibration data of coumarin and 7OH-coumarin analysis are shown in Table 3.13. The measurement of hydroxycoumarin isomers of 3OH-, 4OH-, 5OH-, 6OH- and 8OH-coumarin were also used the calibration equations of 7OH-coumarin. Table 3.14 shows the retention time of the isomers of OH-coumarin.

Table 3.13 Summaries of the calibration equations for coumarin and 7OH-coumarin.

Coumarin		**7OH-coumarin**	
Concentration (mg/L)	Peak Area	Concentration (mg/L)	Peak Area
0	397,840*	0	153,454*
1	439,321*	0.5	324,934*
2	562,533*	1	412,424*
3	705,036*	2	752,419*
4	848,241*	3	1198,654*
5	965,838*	4	1528,125*
10	1515,838*	5	2129,156*
15	2015,838*	10	4436,378*
20	2516,838*	15	6384,175*
Calibration equation:		**Calibration equation:**	
Y = 109,303x + 372,722		Y = 427,382x + 1194	
$\mathbf{R^2}$ = 0.997		$\mathbf{R^2}$ = 0.997	
MDL** (mg/L) = 0.01		**MDL**** (mg/L) = 0.02	

*n = 7

**MDL: Select a concentration which is slightly higher than the lowest concentration in calibration curve and make 7 replicate analysis. 3-times standard deviation (the data of 7 replicate analysis) in terms of concentration unit is the MDL value.

Table 3.14 The retention time of the isomers of OH-coumarin

Isomers of OH-coumarin	**Retention time (minutes)**
3OH-coumarin	19.6 ± 0.15
4OH-coumarin	20.1 ± 0.15
5OH-coumarin	20.4 ± 0.15
6OH-coumarin	21.2 ± 0.15
7OH-coumarin	22.3 ± 0.15
8OH-coumarin	23.9 ± 0.15

n=7

3.3.8 Fourier Transform Infrared Spectrometer (FTIR)

Spectra of the FTIR are obtained using the FT-IR 460 plus analyzer (Jasco Co.). After grinding the freeze-dried sample powder and mixing with potassium bromide (KBr) at weight ratios of (1: 100-200), the sample was pressurized to form a transparent thin slice. The transmittance spectrum was scanned over the wave number from 400 to 4,000 cm^{-1} and then processed using KnowItAIR Information System 3.0 (Bio-Rad Laboratories, Inc.) software transformation to display the spectrum.

3.3.9 Carbon Nuclear Magnetic Resonance (CPMAS 13C NMR)

CPMAS ^{13}C NMR experiments were carried out using a Bruker AVANCE 400 spectrometer operated at a frequency of 100.63 MHz for ^{13}C nucleus under a constant temperature of 300K throughout all experiments. The analysis is supported by Instrument Center at Tsinghua University, Hsinchu, Taiwan.

Operating condition as follows:

1. Operating frequency: 100.48 MHz for ^{13}C nucleus.
2. Recycle delay time: 5 sec.
3. 90° pulse width for 1H excitation was 4 μsec, which corresponds to a $B_{1,H}$ field strength of 60 KHz.
4. Contact time of 1.5 msec.
5. Acquisition time 0.034 sec.
6. Spectral width 303 ppm.
7. Number of scans 80,000 magic angle spinning frequency was consistently used as reference frequency for both the carbon and proton spectra.

Chapter 4 Results and discussion

4.1 Water quality of Te-Chi Reservoir

The main pollutant source of Te-Chi Reservoir was the fertilizer overflowing from agricultural farms and mudslide from steep excess developing mountainside. Over a long time of using organic fertilizer caused the cumulative of nitrides and phosphates in water body. The torrential rain erosion brought these nutrients into water body and stimulates the excess growth of algae, e.g., green and blue green algae. Typically the eutrophication generates algae blooming (red tide) in Reservoir and may cause toxicity of drinking water and odor problems after chlorination.

Table 4.1 is the summary of some water quality parameters of Te-Chi Reservoir raw water between 1996 and 2004 obtained in this study and previous reports. During this period, pH of Te-Chi Reservoir tends to be base obviously from 6.8 to 9.1. The reason may be an excess growth of algae which consume CO_2 in water body. The range of temperature is from 15.8 to 24.1℃. The higher temperature leads to the higher formation of THMs. On July 2, 2004, Mindulle typhoon made a heavy flood disaster,

which caused DO value dropping significantly. In this study, water sample from Te-Chi Reservoir was collected on Sept. 30, 2004. Before it there were several tropical typhoons occurred between July and September, 2004. The possible reason is erosion of topsoil which carried nutrients (fertilizer and insecticide) into Reservoir and causes the excess growth of algae which reduced DO in water. Therefore, the measured DO value is low (5.2 mg/L), which is obviously the lowest one among recent years (Table 4.1). The higher COD value means the more organic materials in water and tends to increase the growth potential of algae in Te-Chi Reservoir. Large amounts of algae generate NOMs and significantly degrade the water quality of Te-Chi Reservoir. When DOC enters a water treatment plant, it will react with chlorine and form DBPs. Therefore, the DOC value is an important index in the water quality. Due to several heavy typhoons invaded with in 3 months before sampling, there were many floating wood in the Reservoir. The floating wood contains organic carbon which may decay and dissolve in water body and caused the highest DOC level (4.76 mg/L) in recent years. Alkalinity is the quantity which can neutralize acids in water and usually express in terms of OH^-、CO_3^{2-} and HCO_3^-. After a serious earthquake occurred on September 21, 2000, tremendous amounts of mud slide scoured into the Reservoir. They are carbonate containing Ca、Mg、Na、K

hydrolyze with acidic carbonate in soil, which will produce excess OH radical and alkalinity. In general, the alkalinity affects the taste of drinking water, and it drops significantly in recent two years (from 113 to 30 mg as $CaCO_3$/L). The hardness (153 mg as $CaCO_3$/L) is higher than the Taiwan EPA drinking water source standard (150 mg as $CaCO_3$). Higher hardness may increase the formation of scale during boiling water. The scale does not only consume energy but also decrease consumer drinkability.

Table 4.1 The water quality parameters of Te-Chi Reservoir raw water in recent years.

Item	**pH**	**Temp**	DO	**TDS**	**COD**	**DOC**	**Conductivity**	**Hardness**	**Alkalinity**	**NH_3-N**
Unit		**℃**	**mg/L**	**mg/L**	**mg/L**	**mg/L**	**μs/cm**	**mg as $CaCO_3$/L**	**mg as $CaCO_3$/L**	**mg NH_3-N/L**
Taiwan EPA std.	6.0-8.5	-	≧6.5	≦250	≦25	≦4	-	≦150	-	≦0.1
1996	9.1	19.8	9.9	323	-	4.07	266	133	200	0.06
1997	7.7	20.3	5.9	145	12	1.40	97	87	130	0.04
1998	7.8	15.8	7.8	-	4	1.53	228	-	-	-
1999	8.7	24.1	8.7	177	-	2.37	196	113	150	0.12
2000	6.8	16.8	8.2	118	-	2.34	241	122	250	-
2001	8.0	23.0	8.3	106	12	1.03	240	94	81	0.36
2002	7.6	20.4	6.5	139	15	2.04	282	163	113	0.08
2003	8.5	22.6	5.8	164	13	0.80	333	160	25	0.05
This study, 2004	8.3	23.4	5.2	138	15	4.76	276	153	30	0.07

In this study, XAD-8 was applied to extract the NOMs and obtained five of organic fraction for investigating the distribution of NOMs. These five species include: HAs, FAs, hydrophobic bases, hydrophobic neutrals and hydrophilic fractions. Figure 4.1 shows the percentage of five organic species separated from Te-Chi Reservoir in 2004. The percentages of hydrophilic and hydrophobic fractions are 40.4% and 59.6%, respectively. The hydrophobic fractions are traditionally described as complicated polyelectrolyte compounds, which can be utilized by microorganism easily. White et al. (2003) cited the higher percentage of hydrophobic fractions in water body, the easier removal efficiency in flocculation process was found. Marhaba and Van (2000) proposed that hydrophobic fractions are the main source to generate DBPFP. Hydrophobic fractions include HAs, FAs, hydrophobic neutrals and hydrophobic bases. In this study, the percentage of HAs, FAs, hydrophobic neutrals and hydrophobic bases are 24.3%, 7.9%, 25.2% and 2.2%, respectively.

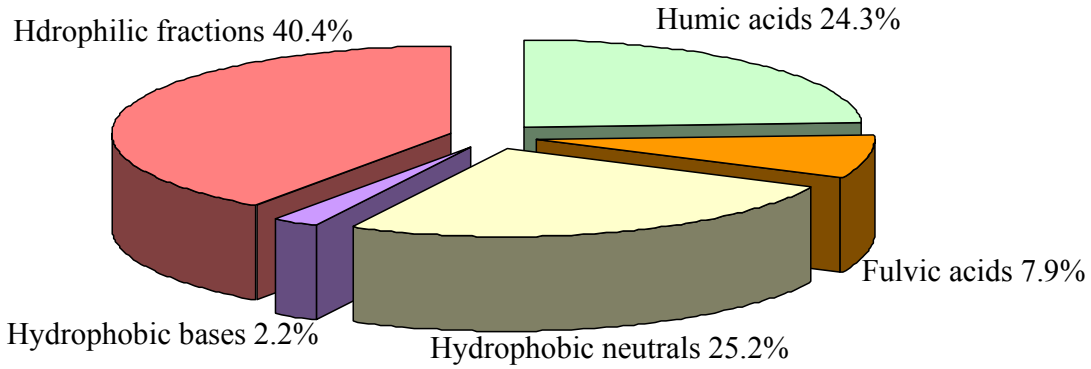

Figure 4.1 The percentage of five species of organic fractions separated from Te-Chi Reservoir in 2004.

In water body, the source of hydrophilic fractions contains the product from algae metabolism and artificial pollution. The more hydrophilic fractions mean the more portions domestic waste water pollution contains. Hydrophilic fractions, which are the minor precursor of DBPFP, are the simple chemical structure can be utilized easily by microorganism.

Table 4.2 shows the percentage distribution of Te-Chi Reservoir NOMs in recent years and compared with other literatures. On July 2, 2004, Mindulle typhoon brought heavy mud slide and tree into Te-Chi Reservoir, the water body contained a lot of hydrophobic matters degraded by tree. HAs content increased significantly after several invasions of typhoons. Comparing with the recent references (Table 4.2), the

percentages of HAs and FAs increase obviously. The different with recent references is the sampling situation. In this study, because there were many floating wood, the HAs and FAs may be higher than the previous references. This is the main reason of higher hydrophobic fractions (59.6%) than hydrophilic fractions (40.4%) in this study. The more hydrophobic fractions in water, the more DBPFP may be generated during the disinfection process. The investigation of Dilling and Kaiser (2002) showed the NOMs' distribution of hydrophilic and hydrophobic fractions is 37% and 63% respectively in Norway's forest area. This means the water body does not contaminated by the artificial pollution. The report of Kitis et al. (2002) cited that the water treatment plant, in Myrtle Beach, South Carolina, USA, did not polluted by the sewerage (hydrophilic fractions 34% and hydrophobic fractions 66%). Marhaba et al. (2000) proposed the percentage of hydrophilic and hydrophobic fractions are 71% and 29% respectively in Passaic Valley WTP, USA. Compare to Te-Chi Reservoir, the NOMs' distribution of hydrophilic and hydrophobic fractions are 40.4% and 59.6% respectively. The value of hydrophilic fractions is the highest among the data obtained from Dilling and Kaiser (2002) and Kitis et al., (2002). This is due to the NOMs generated by algae blooming which are polluted by the artificial substance.

Table 4.2 The percentage distribution of Te-Chi Reservoir NOMs (% of DOC) in recent years and comparison of literatures.

Reference,Fraction (%)	HA	FA	Hydrophobic neutrals	Hydrophobic bases	Hydrophilic fractions
1999	7.6	11.6	25.4	1.5	45.8
2000	8.5	14.4	-	77.0	-
2001	7.5	11.3	24.1	1.4	55.5
2002	8.0	11.0	26.0	1.0	53.0
2003	10.0	11.6	26.0	1.6	49.5
This study, 2004	24.3	7.9	25.2	2.2	40.4

	Hydrophobic fractions	Hydrophilic fractions
Dilling and Kaiser (2002), Forest floor, Norway	63	37
Kitis et al. (2002), Myrtle Beach, South Carolina,USA	66	34
Marhaba et al. (2000), Passaic Valley WTP,USA	29	71

White et al. (2003) cited that the ratio of UV_{254} and DOC is referred to the specific ultraviolet absorbance (SUVA) and is used to represent the enrichment of DOC in DBP precursors. A relatively low SUVA did not enrich in DBP forming precursors. Figure 4.2 shows the profiles of SUVA (Specific ultra-violet absorbance, A_{254}/DOC) for raw water and five organic fractions (HAs, FAs, hydrophobic bases, hydrophobic neutrals and hydrophilic fractions) extracted from Te-Chi Reservoir. The specific absorbance value of hydrophobic fractions is higher than hydrophilic fractions. Among hydrophobic fractions, HAs (0.019 abs/ mg) and FAs (0.010 abs/ mg) show the higher value than other species. Goel et al., (1995) indicates the content of unsaturated bond in HAs and FAs is higher than other fractions. On the contrary, SUVA of hydrophilic fractions is less than 0.007 abs/ mg, which indicate the content of unsaturated bond is low. Goel et al. (1995) proposed that the higher A_{254} in organic matter, the more unsaturated bond structure, i.e., C=C or aromatic, exists. Kitis et al. (2002) also cited the SUVA value of hydrophobic fraction (0.046 abs/ mg) is higher than that of hydrophilic fraction (0.020 abs/ mg) in water treatment plant in South Carolina, Myrtle Beach, USA.

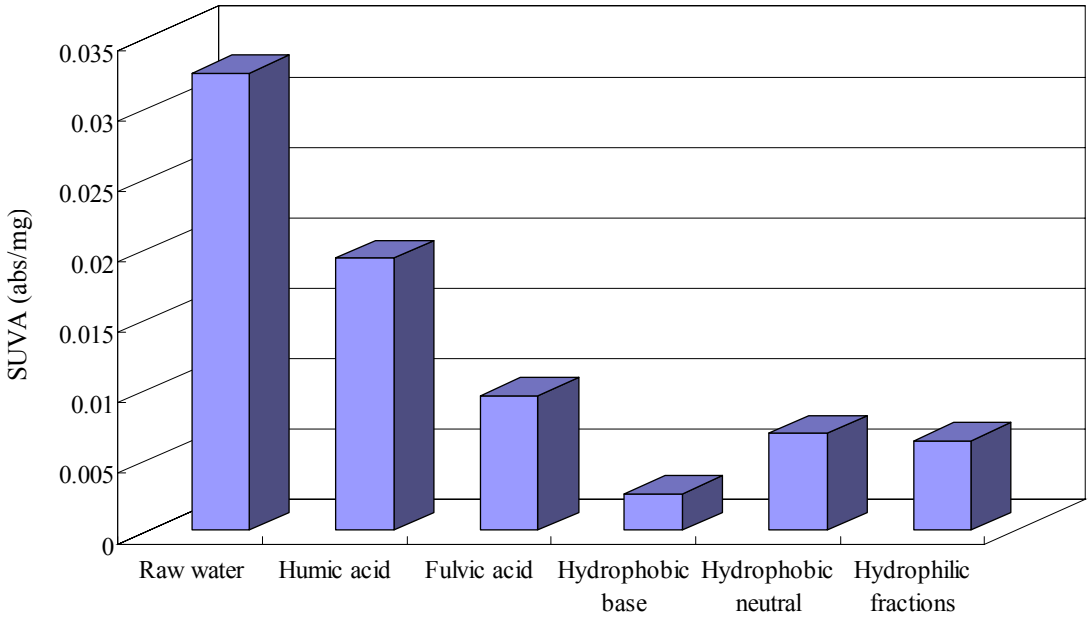

Figure 4.2 The SUVA value (A_{254}/DOC) of raw water and five fractions (HAs, FAs, hydrophobic bases, hydrophobic neutrals and hydrophilic fractions) extracted from Te-Chi Reservoir in 2004.

Figure 4.3 displays the DBPFPs/DOC of various organic fractions extracted from Te-Chi Reservoir. Table 4.3 shows the comparison of TTHMFP/DOC, HAAFP/DOC, AOXFP/DOC and (AOXFP/DOC) / [(THMFP /DOC) + (HAAFP /DOC)] for five species obtained from literature and this study. The experiment result showed the HAs and FAs' formation potentials of TTHMFP/DOC were higher than other organic fractions. Among all, the TTHMFP/DOC value of FAs (50.7 μg/mg) is the highest while the second is HAs (38.6 μg/mg). Therefore, it is supposed

that HAs and FAs (both are the hydrophobic acids) may be the main precursors to generate TTHM. Meanwhile, the TTHMFP/DOC ratios of FAs are 3.11, 6.26 and 3.43 times of hydrophobic neutrals (16.3 μg/mg), hydrophobic bases (8.1 μg/mg) and hydrophilic fractions (14.8 μg/mg) respectively. The TTHMFP/DOC of hydrophobic fractions is 7.68 times more than that of hydrophilic fractions and the ratio is close to the data obtained at 1999 and 2001 (both all 7.23 times).

The HAAFP/DOC value in FA (53.0 μg/mg) is the highest while the second is HA (42.0 μg/mg). HAAFP/DOC of FA are the 1.86, 2.86 and 1.3 times of hydrophobic neutrals (28.5 μg/mg), hydrophobic bases (18.5 μg/mg) and hydrophilic fractions (40.9 μg/mg) respectively. TTHMFP/DOC and HAAFP/DOC of the Te-Chi Reservoir raw water are 19 and 34 μg/mg (Figure 4.3). In all, the hydrophobic fractions, which contain the fractions of HA, FA, hydrophobic neutrals and hydrophobic bases, are the major precursor of TTHMFP/DOC and HAAFP/DOC. As for AOXFP/DOC, the value generated by hydrophilic fractions is higher than that of hydrophobic fractions. Among all species, the AOXFP/DOC has a trend of: hydrophilic fractions ＞ hydrophobic bases ＞ hydrophobic neutrals ＞ FAs ＞ HAs. This trend is similar to those reports cited previously. It means that beside of TTHM and HAA, these many other organic halide compounds may also

generate DBPs. The AOX covers the overall output absorbance organics in water, which are much more than that of THMs and HAAs. In this study, the ratios of (THMFP+HAAFP)/(AOXFP) are between 0.1 and 0.95. Ko et al. (2000) cited that the ratios of river water (river Ruhr, Essen) of (THMFP+HAAFP)/(AOXFP) are 0.87 ((21.5+56)/89.2), 0.58 ((9.52+28)/64.6) and 0.59 ((4.12+28)/54.3) through chlorination, preozonaiton (3.5 mg/L) + chlorination and preozonaiton (12.5 mg/L) + chlorination respectively.

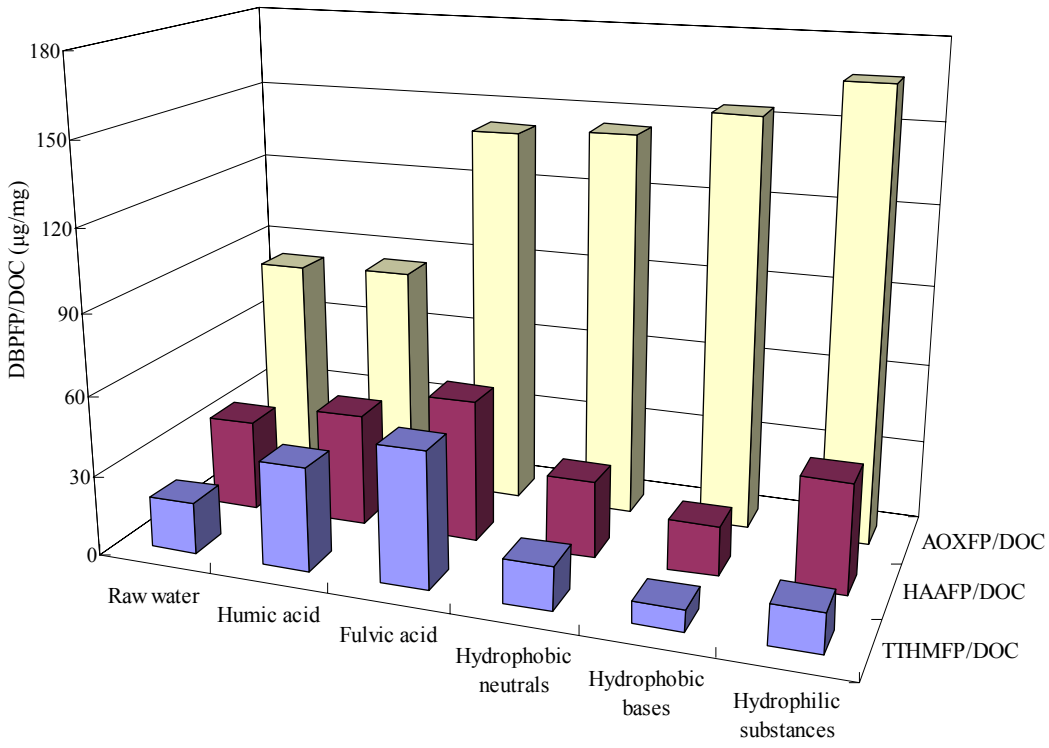

Figure 4.3 The DBPFPs/DOC of raw water and five organic fractions (HAs, FAs, hydrophobic bases, hydrophobic neutrals and hydrophilic fractions) extracted from Te-Chi Reservoir in 2004.

Table 4.3 Comparison of TTHMFP/DOC, HAAFP/DOC, AOXFP/DOC and (THMFP+HAAFP)/(AOXFP) (HAs, FAs, hydrophobic bases, hydrophobic neutrals and hydrophilic fractions separated from Te-Chi Reservoir) obtained from literatures and this study.

literatures	HA	FA	Hydrophobic neutrals	Hydrophobic bases	Hydrophilic fractions
1999					
TTHMFP/DOC (μg/mg)	24.7	47.1	12.7	5.9	12.5
AOXFP/DOC (μg/mg)	83.3	195.5	180.2	210.6	446.1
2001					
TTHMFP/DOC (μg/mg)	24.7	47.1	12.7	5.9	12.5
AOXFP/DOC (μg/mg)	83.0	195.0	180.0	210.0	444.0
2002					
TTHMFP/DOC (μg/mg)	36.4	46.7	15.0	8.0	18.5
HAAFP/DOC (μg/mg)	37.9	71.4	24.1	18.2	80.3
AOXFP/DOC (μg/mg)	87.4	137.6	145.3	195.0	418.3
(THMFP+HAAFP)/(AOXFP)	0.85	0.86	0.27	0.13	0.24
2003					
TTHMFP/DOC (μg/mg)	35.7	22.2	10.7	5.9	2.9
HAAFP/DOC (μg/mg)	28.2	47.8	21.3	16.7	7.6
AOXFP/DOC (μg/mg)	80.0	91.2	111.7	120.0	107.6
(THMFP+HAAFP)/(AOXFP)	0.80	0.77	0.29	0.19	0.10
This study, 2004					
TTHMFP/DOC (μg/mg)	38.6	50.7	16.3	8.1	14.8
HAAFP/DOC (μg/mg)	42.0	53.0	28.5	18.5	40.9
AOXFP/DOC (μg/mg)	84.5	142.0	144.3	153.8	354.2
(THMFP+HAAFP)/(AOXFP)	0.95	0.73	0.31	0.17	0.16

4.2 The investigation of direct and indirect ozonation

Ozone, which is one of the most popular advanced oxidation processes (AOPs), is recognized to decompose DBPs effectively in water (Kleiser and Frimmel, 2000, Von Gunten, 2003a and Von Gunten, 2003b). Many literatures showed ozone reaction contains two steps, direct (ozone molecular) and indirect (free hydroxyl radicals) attack. The mechanisms can be investigated by adding scavenger to quench free hydroxyl radicals (Staehelin and Hoigné, 1982; Benitez et al., 1994; Chu and Ma, 2000; Chu and Ching, 2003). It is difficult to measure free hydroxyl radicals due to its short half-life, which estimated to be around 10^{-9} s (Sarma et al., 1996). Due to the presence of an unpaired electron, free radicals are highly unstable and immeasurable. Recently, many researchers proposed the analysis of free radicals successfully (Nakao et al., 1999 and Utsumi et al., 2003).

This study adapts HPLC trap to measure free hydroxyl radicals by adding coumarin as quenching agent. Coumarin is a molecule that has been known to form the fluorescent 7–hydroxycoumarin by reaction with hydroxyl radicals in aqueous solutions, shown in Eq 4.1 (Louit et al., 2005).

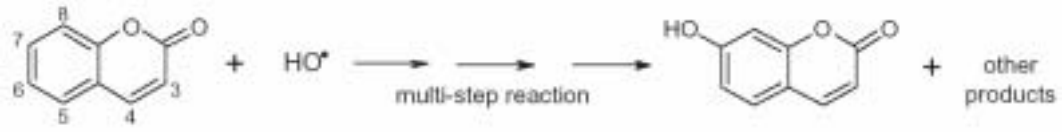

…..Eq. 4.1

Louit et al. (2005) also indicated that the hydroxycoumarin isomers of 3OH-, 4OH-, 5OH-, 6OH- and 8OH-coumarin are also produced during the ozonation with coumarin. HPLC can detect the whole hydroxycoumarin and therefore, the free hydroxyl radicals can be measured indirectly. This study purges ozone to pure water until the saturated level then doses various concentrations (0-20 mg/L) of coumarin into the reactor. When the on-line measured ozone drops to null, the sample was taken to measure the consumed coumarin concentration. Figure 4.4 showed the consumed coumarin concentration (mg/L) vs. the initial addition coumarin concentration (mg/L), the optima concentration of adding coumarin can be found. Pure water is selected to react with ozone, because pure water will produce the most amount hydroxyl radicals, which can not react with other organic compounds. Figure 4.4 shows the suitable dosage of coumarin is 18 mg/L. The over dose of coumarin does not enhance the effect of trapping hydroxyl radical any more.

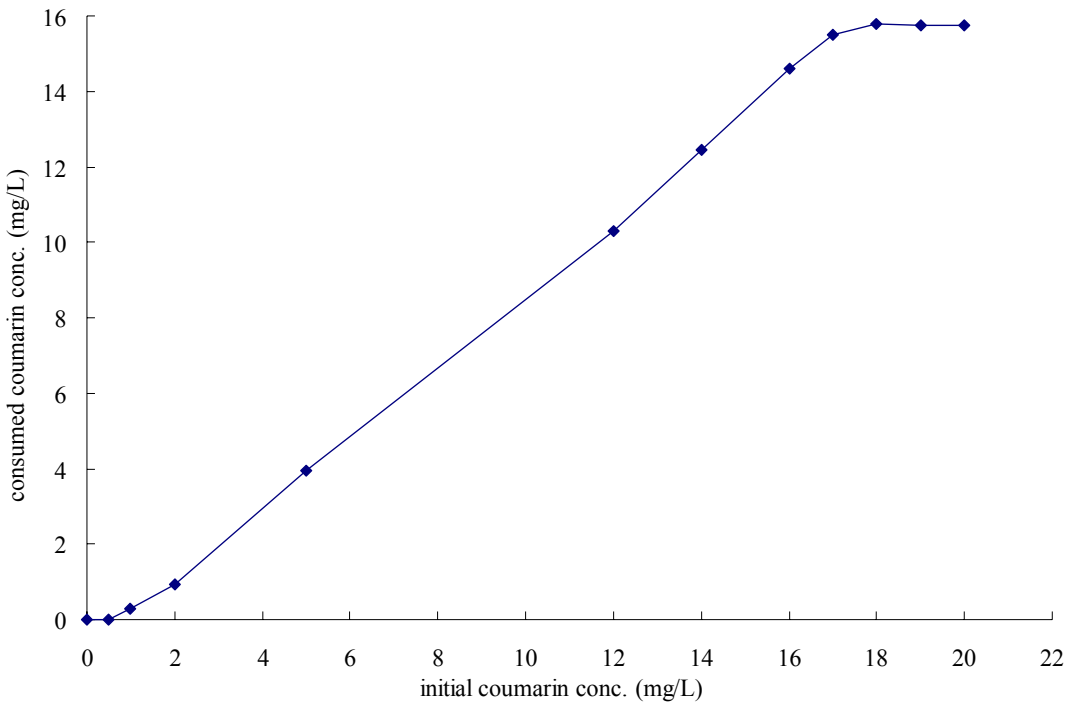

Figure 4.4 The consumed coumarin concentration (mg/L) vs. the initial addition coumarin concentration (mg/L) in pure water until DO_3 = 0 mg/L.

Carbonate and bicarbonate substance are well-known radical scavengers (Hoigné and Bader, 1985). In this study, carbonate/bicarbonate solution is used as a quenching agent to capture the indirect free radical generated by ozone so that indirect hydroxyl radical oxidation is suppressed. Pi et al. (2005) also cited that scavenger can inhibit the chain reaction of some aromatic compounds by consuming hydroxyl radicals. Figure 4.5 shows the consumed coumarin concentration (mg/L) of the scavenger

concentration (mg/L) in blank (pure water) until DO_3 (dissolved ozone concentration) = 0 mg/L. The non-inhibited oxidation is showing with 0 mg/L carbonate/bicarbonate addition (or control test), which combined indirect hydroxyl radical oxidation and direct molecular ozone oxidation removes 15.64 mg/L coumarin. The test result shows the 5 mg/L of scavenger can significantly provide inhibition effect on the free radicals inhibited. The consumed coumarin appears to decrease with the addition carbonate/bicarbonate scavenger during ozonation (Figure 4.5). Wang et al. (2004) also cited that the increase of the concentration of scavenger, the depletion rate of ozone (coumarin) decreases.

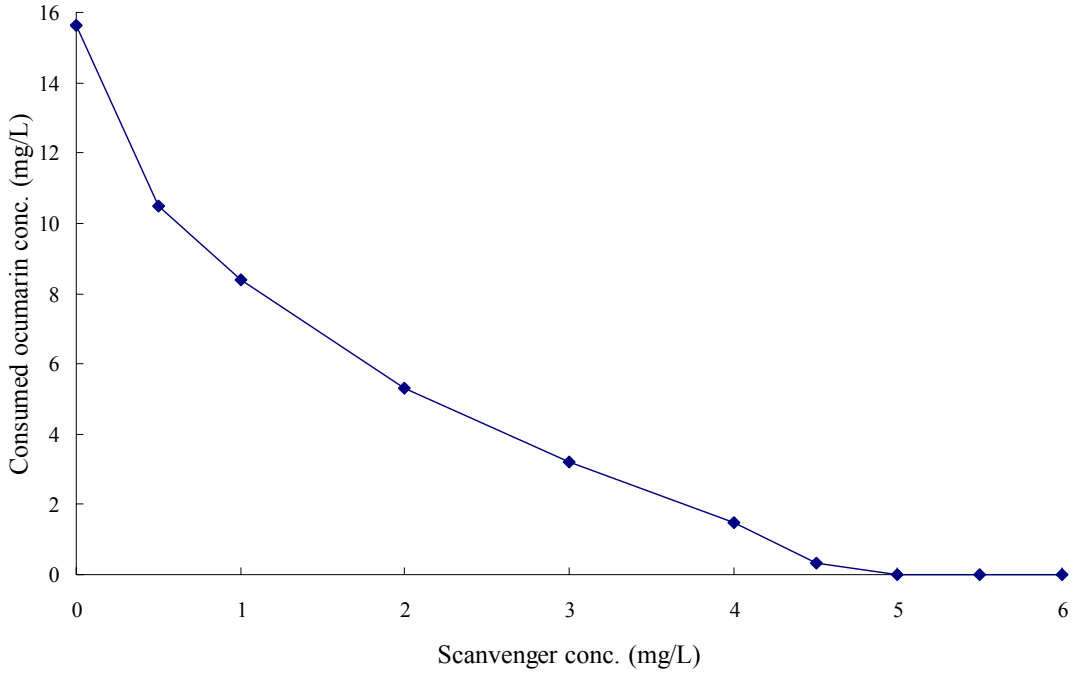

Figure 4.5 The consumed coumarin concentration (mg/L) of the theoretical maximum scavenger dosage in ozone blank is 5 mg/L concentration (mg/L) in blank test (pure water) when DO_3 = 0 mg/L.

In this study, on-line dissolved ozone, ORP and pH system is used to monitor the comprehensive reaction profiles. Figure 4.6 shows the analytic values (ORP, pH DO_3 and hydroxyl radicals) in ozone degradation of Te-Chi Reservoir raw water. Due to the indirect measurement of hydroxyl radicals, the hydroxyl radicals are measured by the hydroxyl radicals quantity of pure water subtract the hydroxyl radicals' quantity of coumarin trapping in reactor. Therefore, the hydroxyl radicals' value in Figure 4.6 means the reacted

quantity with organic compounds. In which the ozone is aerated to saturation, i.e., at the 150 seconds, the DO_3 reaching saturate (2.8 mg/L). After 150 seconds, the aerated ozone is stop in order to investigate the residue ozone reaction. In Te-Chi Reservoir raw water test, the DO_3 decreased gradually, due to the decomposition of NOMs and the production of hydroxyl radicals. Meanwhile, hydroxyl radicals decreased when DO_3 dropped, i.e. the indirect reaction with NOMs. About 2,500 seconds, the DO_3 and hydroxyl radicals consumed completely. The NOMs in water are oxided by ozone molecular and hydroxyl radicals, while in pure water, without NOMs, the level of dissolved ozone DO_3 is seldom to be consumed. Over 2 hrs, ozone in the pure water system disappears completely, because ozone is unstable and has vaporized (Figure 4.7). In raw water ozone test, ORP value increase rapidly at first then the DO_3 is saturated in water, the ORP profile drops gradually and keeps stable situation till end. At 2,500 second, the ORP decreases significantly, it is because of the running out of ozone and hydroxyl radicals. At the same time the redox reaction is less progressively and can be found by the decrease of ORP value. After the disappeared of DO_3, then hydroxyl radicals, ORP value drops rapidly. The pH value does not change obviously and within the range between 7.8 and 8.5.

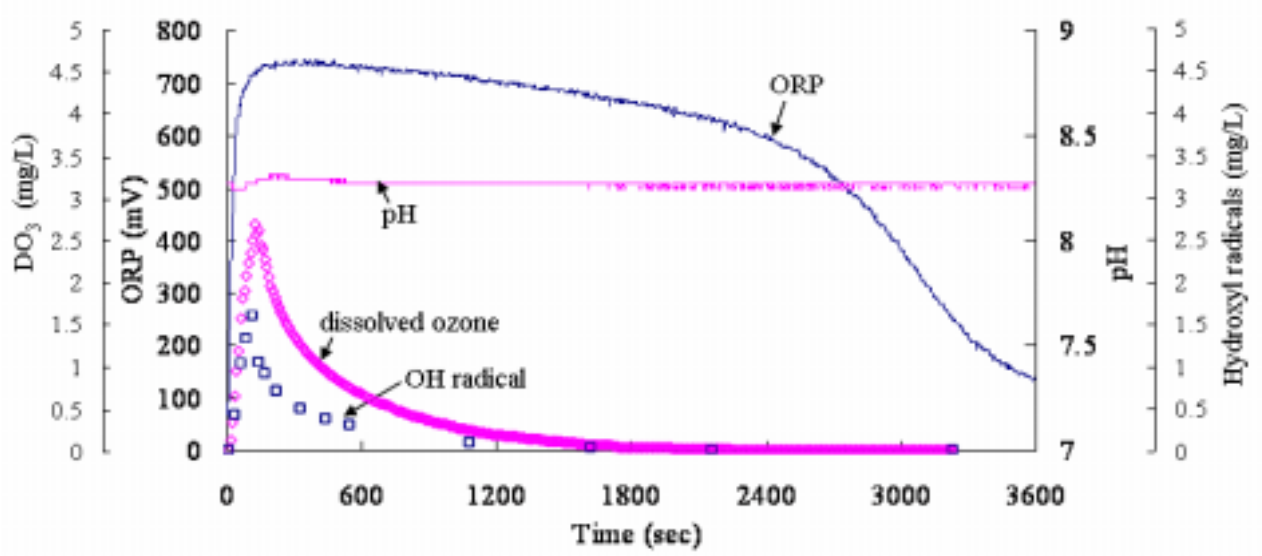

Figure 4.6 the analytic values (ORP, pH, DO_3 and hydroxyl radicals) in ozone degradation of Te-Chi Reservoir raw water

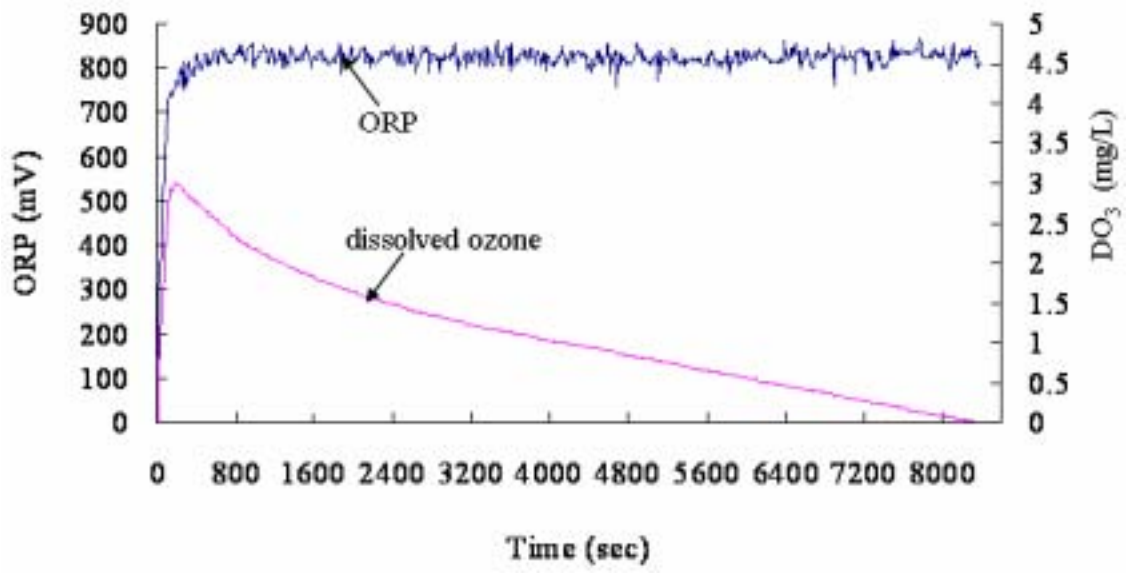

Figure 4.7 the analytic values (ORP and DO_3) in ozone degradation of pure water

Figure 4.8 shows the analytic values (ORP, pH DO_3 and hydroxyl radicals) in ozone degradation of Te-Chi Reservoir raw water with quenching inhibition. The hydroxyl radicals are inhibited by the dosing of 5 mg/L scavenger (carbonate and bicarbonate). The DO_3 react reach to the peak at 90 second and then the purge of ozone to system is stopped (Figure 4.8). Compared with Figure 4.6, the system without inhibitor, the ozone and hydroxyls radical are last 2,500 seconds, which are much longer than the inhibited test (Figure 4.8). The DO_3 and hydroxyl radicals are disappeared at 480 second and 90 seconds, respectively. Hydroxyl radicals disappear immediately when the scavenger is adding to the reactor. The drop of ORP value is also very steady to the end. The pH value was lift from 7.0 to 9.2 when the scavenger is added. The scavenger inhibits hydroxyl radicals and causes the ORP changes. Since scavenger (carbonate and bicarbonate) is recognized as a buffer solution, and with final pH value of 9.2 (McGhee, 1991). Therefore, the ozonation of direct and indirect reaction can be preliminary clearly investigated (Acero et al., 2003).

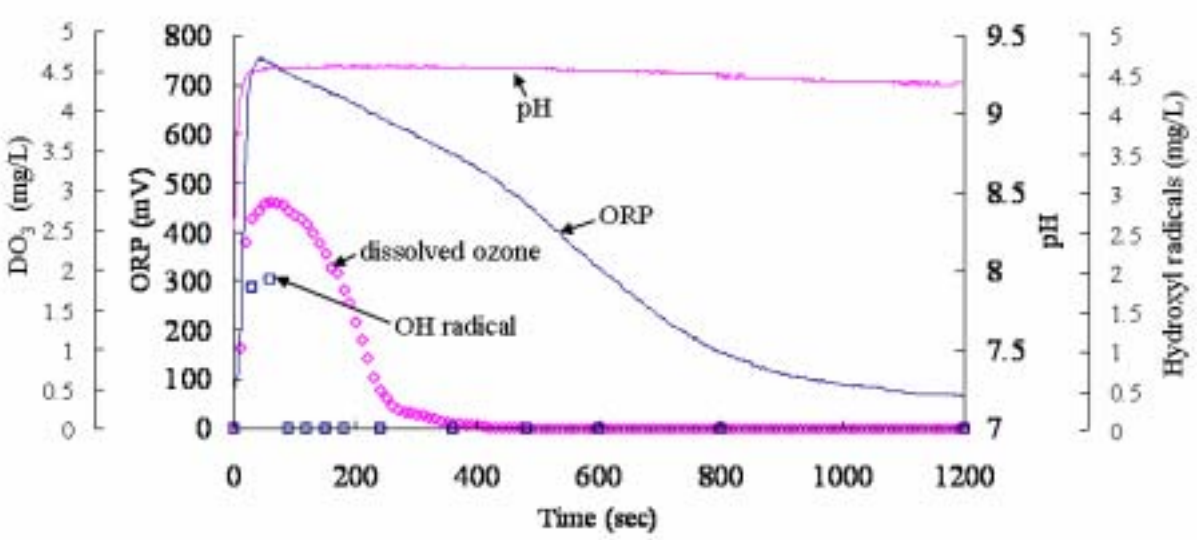

Figure 4.8 the analytic values (ORP, pH, DO_3 and hydroxyl radicals) in ozone degradation of Te-Chi Reservoir raw water with quench inhibition test.

Figure 4.9 shows the comparison of the ORP profiles with and without inhibition. At 480 seconds, the DO_3 and hydroxyl radicals are 0 mg/L in inhibited system. From the cross point (120 seconds) to 480 seconds, the ORP area of without inhibit subtracts the ORP area of reactor with inhibition implies the area reacted by indirect reaction (hydroxyl radicals). After 480 seconds, the ORP area of without inhibit subtracts the ORP area of with inhibit means the area caused by indirect (hydroxyl radicals) and direct reaction (ozone molecular). The dosing of scavenger caused the inhibition of hydroxyl radicals. The detail redox reaction is not clear and need to be discussed in future. The area of ORP vs. reaction time may be able to help investigated and illustrating the ozone reaction mechanisms.

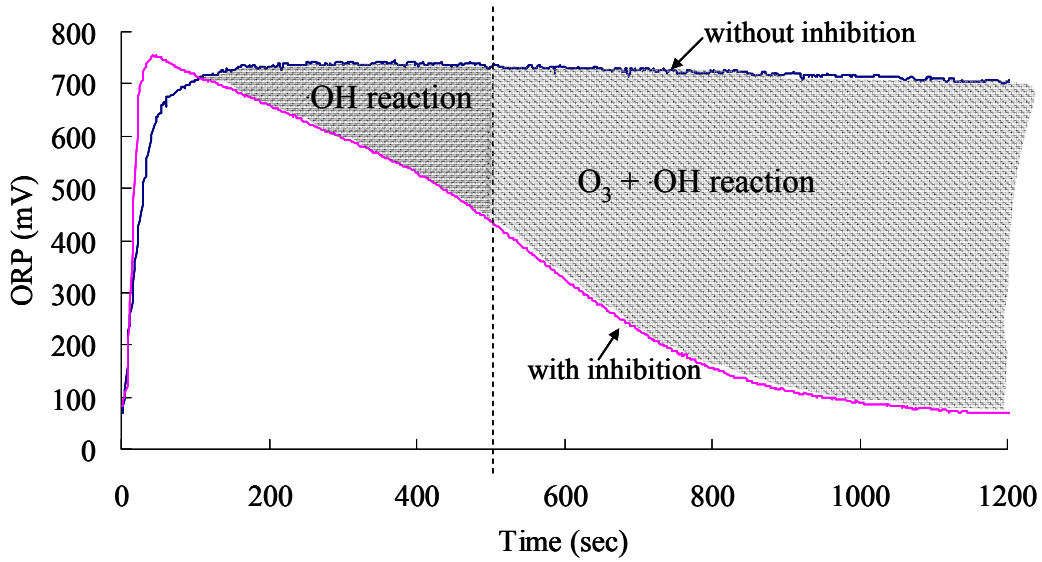

Figure 4.9 The comparison of ORP profile with inhibit dose quenching 5mg/L and without inhibit under ozonation with Te-Chi Reservoir raw water.

4.3 Nernst model simulation and application

Nicoli et al. (2004) cited that The ORP value gives information about the real oxidation/reduction ability of a molecule and its prevalent form (oxidized or reduced) in the system. The Nernst equation has been widely used to simulate oxidation/reduction reactions and can display as standard form:

$Oxi + n\ e^- \rightarrow Red \qquad E^0$

$E = E_0 - RT/nF\ \ln([Red]/[Oxi])$…….Eq. 4.2

Where, $n\ e^-$ = n mole electron

E = the electrode potential of chemical reactions (mV)

E_0 = the standard electron potential (mV)

R = gas constant (8.314 V-coulombs K^{-1} mol^{-1})

T = the absolute temperature (K)

n = the number of electrochemical gram equivalent per gram mole exchanged during the redox reaction (equivalent mol^{-1})

F = Frarday's constant (96,500 coulombs $equivalent^{-1}$)

[Oxi] = oxidizing agent

[Red] = reducing agent

Nernst equation is used for general redox reaction. A general redox reaction can be represented as Eq. 4.3 (Barrow, 1988):

$aA + bB \leftrightarrow cC + dD$ ……..Eq. 4.3

Where A and B are reactants; C and D are products; and a-d are the stoichiometric coefficients for species A-D, respectively. All species involved in the chemical reaction are assumed to be dissolved solutions. If solids are involved in the reaction, their concentrations are assumed unchanged during the reaction. Similarly, if the reagent is a pure substance rather than the component of a solution, the partial molar free energy equals to the free energy with 1 mol of the substance. The Nernst equation for a generalized oxidation-reduction reaction is obtained:

$$E = E^0 - \frac{RT}{nF}\ln\frac{(a_C)^c(a_D)^d}{(a_A)^a(a_B)^b} \quad \text{or} \quad E = E^0 + \frac{RT}{nF}\ln\frac{(a_A)^a(a_B)^b}{(a_C)^c(a_D)^d} \text{ ……..Eq. 4.4}$$

Nernst equation is applied for the ozonation process. The main redox reaction is organic compounds convert to CO_2 and H_2O. The chemical redox reaction is expressed by the following generic stoichiometric shown as Eq. 4.5:

$5C_xH_yO_z + O_3 + (40x + 10y - 20z - 12)\cdot OH \rightarrow 5xCO_2 + (10x + 5y - 5z -$

3)$H_2O + (20x + 5y – 10z – 6)OH^-$ .....Eq. 4.5

Applying the generalized Nernst equation, the Nernst equation for the ozonation precess is

$$E = E^0 + \frac{RT}{nF}\ln\left(\frac{\left[C_xH_yO_z\right]^5\left[O_3\right]\left[\cdot OH\right]^{(40x+10y-20z-12)}}{\left[CO_2\right]^{5x}\left[OH^-\right]^{(20x+5y-10z-6)}}\right) \quad \text{.....Eq. 4.6}$$

or $$E = E^0 - \frac{(5x)RT}{nF}\ln\left[CO_2\right] - \frac{(20x+5y-10z-6)RT}{nF}\ln\left[OH^-\right]$$

$$+\frac{5RT}{nF}\ln\left[C_xH_yO_z\right] + \frac{RT}{nF}\ln\left[O_3\right] + \frac{(40x+10y-20z-12)RT}{nF}\ln\left[\cdot OH\right] \quad \text{.....Eq. 4.7}$$

Simplified form is obtained with constants a', b', c and d as defined in the following equations:

$$a' = E^0 - \frac{(5x)RT}{nF}\ln\left[CO_2\right]$$

If hydrogen ion is consumed and leading to an increasing solution pH during the ozone reaction, this can be included in the Nernst Equation as a reactant with water being the product whose concentration is practically unchanged.

$$b' = -\frac{(20x+5y-10z-6)RT}{nF}$$

$$c = \frac{RT}{nF}$$

$$d = \frac{(40x + 10y - 20z - 12)RT}{nF}$$

Then Eq. 4.7 could be simplified as Eq. 4.8:

$$E = a' + b' \ln[OH^-] + c \ln[C_x H_y O_z][O_3] + d \ln[\cdot OH] \quad \text{.....Eq. 4.8}$$

Replacing 2.3026*(pH-14) for ln[OH^-] obtains Eq. 4.9

$$E = a + b\ pH + c \ln[C_x H_y O_z][O_3] + d \ln[\cdot OH] \quad \text{.....Eq. 4.9}$$

Where $a = a' - 32.2364$

$b = 2.3026 * b'$

Theoretically, the concentration of both the original and products can be represented by the measurement of absorbance at 254 nm (A_{254}). The decrease of A_{254} under ozonation implies the unsaturated double bond is reduced. Therefore, organic compounds ($C_xH_yO_z$) can be replaced by A_{254} for detecting decomposed organic compounds. DO_3 and free OH radical can be measured and added to the redox reaction equation. The Nernst equation (Eq. 4.2 and 4.9) can be expressed as Eq. 4.10

$$E = a + b\ pH + c \ln[A_{254}][O_3] + d \ln[\cdot OH] \quad \text{.....Eq. 4.10}$$

During the ozonation, adapt the A_{254} values at different time for treated Te-Chi Reservoir raw water; the following Nernst equation is obtained:

$$ORP = 54 - 62\ pH - 663\ \ln[A_{254}][O_3] + 694\ \ln[{}^{\cdot}OH] \quad \text{Eq. 4.11}$$

The model regression shows a satisfactory R-square value of 0.97.

The preliminary model developed in this study can be one of the redox type models used to simulate the ozonation. Due to there are many different types of target compounds need to be investigated in the future. Therefore, the author suggests set up different types of modified Nernst equation for different cases. Especially for the complicate compounds, the redox reaction may not be able to adapt smoothly.

4.4 Effect of in inhibited and non-inhibited reaction on the change of functional groups

Table 4.4 shows abbreviated tables of group frequencies for organic groups (Calace et al., 1999 and Hafidi et al., 2005). It displays the information of the different wave number range the different chemical bond of chemical compound. It helps to determine and illustrate the FTIR spectrum and investigate the change of functional groups before and after ozonation with scavenger.

Table 4.4 Abbreviated tables of group frequencies for organic groups (Calace et al., 1999 and Hafidi et al., 2005).

Type of compound	Bond	Wave number(cm^{-1})
Alkanes	C-H (stretch)	2,850-2,970
		1,340-14,70
	-CH (Bending)	1,350-1,480
Alkenes	C-H (Stretch)	3,010-3,095
	=CH (Bending)	675-1,000
	C=C (Stretch)	1,610-1,680
Alkynes	C-H (Stretch)	3,300
	C≡C (Stretch)	2,100-2,260
Alcohols	O-H (stretch, H-bonded)	3,200-3,600
	O-H (stretch, free)	3,590-3,650
	C-O (stretch)	1,050-1,300
Alkyl Halide	C-F (Stretch)	1,000-1,400
	C-Cl (Stretch)	600-800
	C-Br (Stretch)	500-600
	C-I (Stretch)	500
Amines, amides	N-H (Stretch)	3,300-3,500
	C-N (Stretch)	1,180-1,360
Aromatic rings	C-H (Stretch)	3,010-3,100
		690-900
	C=C (Stretch)	1,500-1,600
Carboxylic acids	C-O (Stretch)	1,050-1,300
	O-H (Stretch)	3,500-3,600
	O-H (stretch, H-bonded)	2,500-2,700
	C=O (Stretch)	1,690-1,760
Ether	C-O (Stretch)	1,050-1,300
Ester	C-O (Stretch)	1,050-1,300
	C=O (Stretch)	1,690-1,760
Aldehydes, Ketones	C=O (Stretch)	1,500-1,570

Figure 4.10 shows FTIR spectrums of Te-Chi Reservoir raw water during (a) before ozonation, (b) after ozonation with 5 mg/L scavenger and (c) after ozonation. Occurrence of valleys on the transmittance curves are caused by the adsorption or the presence of specific functional groups. The main transmittance peaks are C-Cl and C-Br chemical bonds in alkyl halide (500-800 cm^{-1}), C-H chemical bonds in aromatic rings (810-900 cm^{-1}), C-O chemical bonds in alcohols, ester and ether (1,050-1,300 cm^{-1}), -CH chemical bonds in alkanes (1,350-1,480 cm^{-1}), C=C chemical bonds in alkenes (1,610-1,680 cm^{-1}), N-H chemical bonds in amines and amides (3,300-3,500 cm^{-1}) and O-H chemical bonds in carboxylic acids (3,500-3,600 cm^{-1}). The adsorption valleys occurring during 2,300-2,400 cm^{-1} correspond to carbon dioxide (Chu et al., 1999 and Chien et al., 2000). The FTIR spectrums show three vibrated lines. The vibrated line (a) is used as a base for comparison. Through the comparison of these vibrated lines, the organic compounds could decay as shown in (b) and (c) where an obvious decrease of transmittance was observed. This means the strongly destroy of chemical bonds by the direct (ozone molecular) and indirect (hydroxyl radicals) attack. The reaction of ozonation with scavenger also has the decrease of transmittance. Due to the quenching of hydroxyl radicals, the decrease of transmittance is not as strong as ozone reaction.

Therefore, we can find the NOMs' change of functional group after ozonation from the FTIR spectrum of Te-Chi Reservoir raw water with (b) after ozonation with scavenger and (c) after ozonation.

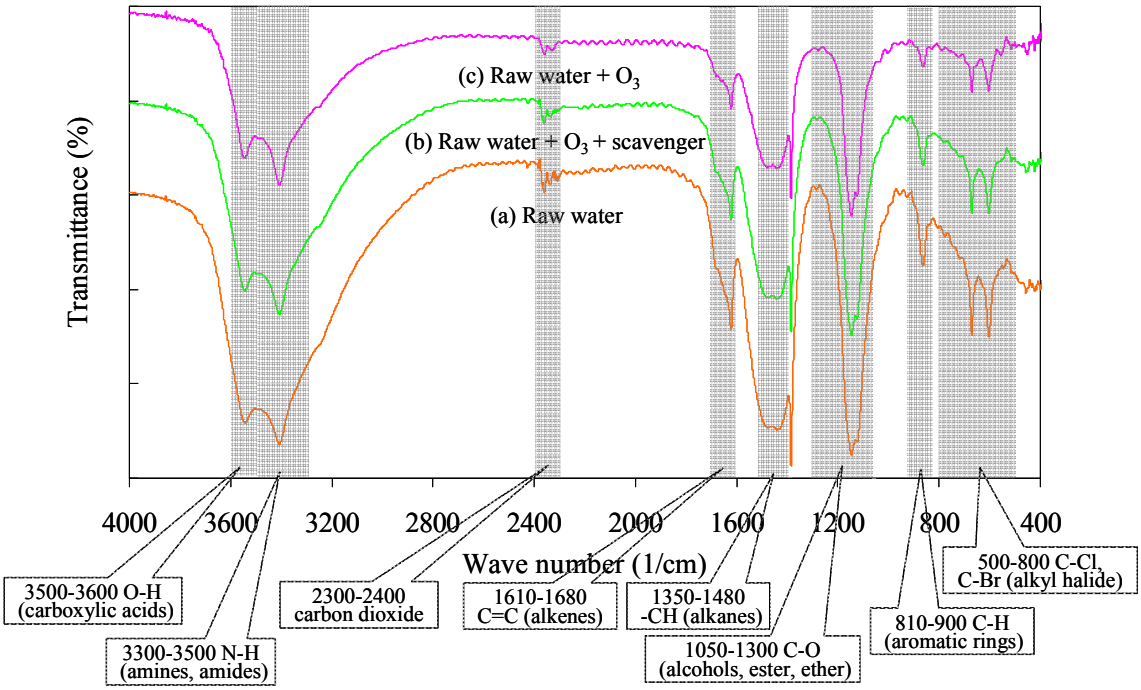

Figure 4.10 FTIR spectrums of Te-Chi Reservoir raw water during (a) before ozonation, (b) after ozonation with 5 mg/L scavenger and (c) after ozonation.

Figure 4.11 shows FTIR spectrums of HAs separated from Te-Chi Reservoir raw water during (a) before ozonation, (b) after ozonation with 5 mg/L scavenger and (c) after ozonation. The vibrated line (a) is used as a base for comparison. Occurrence of valleys on the transmittance curves are caused by the adsorption or the presence of specific functional groups. The main transmittance peaks are C-Cl and C-Br chemical bonds in alkyl halide (500-800 cm^{-1}), C-H chemical bonds in aromatic rings (810-900 cm^{-1}), -CH chemical bonds in alkanes (1,350-1,480 cm^{-1}), C=C chemical bonds in alkenes (1,610-1,680 cm^{-1}) and N-H chemical bonds in amines and amides (3,300-3,500 cm^{-1}). The adsorption valleys occurring during 2300-2400 cm^{-1} correspond to carbon dioxide (Chu et al., 1999 and Chien et al., 2000). Through the comparison of these vibrated lines, an obvious decrease of transmittance was found after ozonation. It means that chemical bonds were strongly destroyed by the direct (ozone molecular) and indirect (hydroxyl radicals) attack. The reaction of ozonation with scavenger also has the decrease of transmittance. Due to the quenching of hydroxyl radicals, the decrease of transmittance is not as strong as ozone reaction. Therefore, we can find the functional groups of NOMs were changed after ozone oxidation reaction from the FTIR spectrum of HAs extracted Te-Chi Reservoir raw water during (a) before ozonation, (b) after ozonation with

scavenger and (c) after ozonation. Comparing with Figure 4.10, the C-O chemical bonds in alcohols, ester and ether (1,050-1,300 cm^{-1}) and the O-H chemical bonds in carboxylic acids (3500-3600 cm^{-1}) are not shown. It means after separated process some chemical bonds would be distributed to different substances. Therefore, the FTIR spectrum of HAs separated from Te-Chi Reservoir (Figure 4.11) does not has the characteristic of some chemical bonds occurred in Figure 4.10. The destruction of ozonation in raw water tends to be stronger than that in HAs.

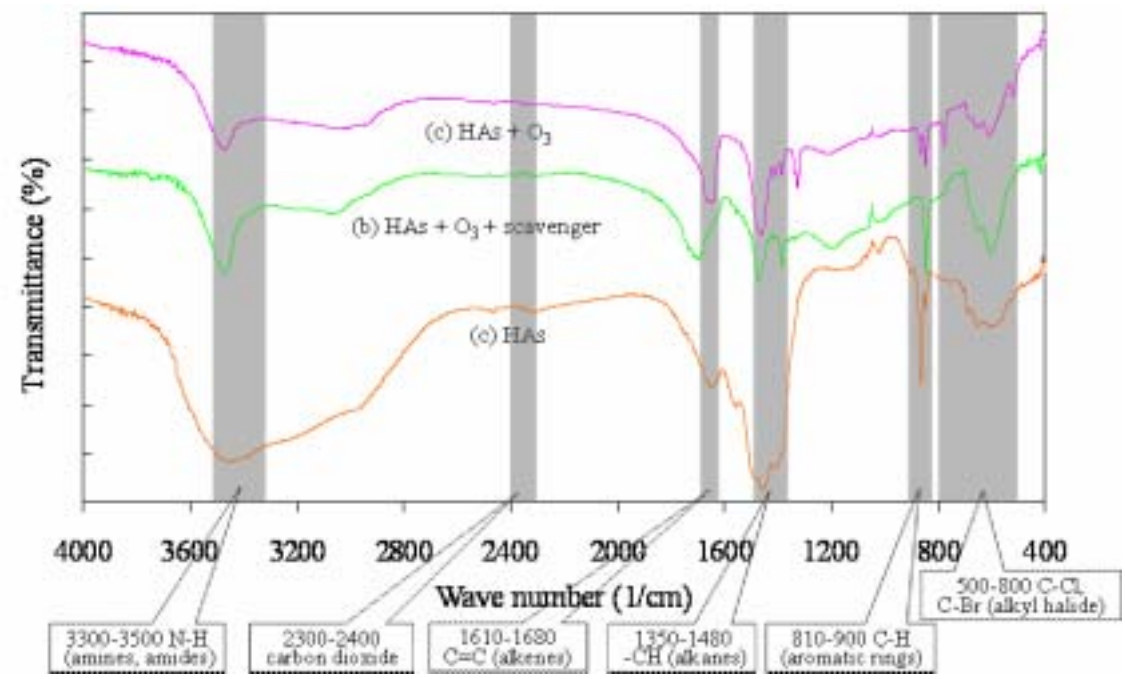

Figure 4.11 FTIR spectrums of HAs extracted from Te-Chi Reservoir raw water during (a) before ozonation, (b) after ozonation with 5 mg/L scavenger and (c) after ozonation.

Figure 4.12 shows ^{13}C NMR spectra of Te-Chi Reservoir raw water. Line (a) is before ozonation; line (b) is after ozonation with scavenger (direct molecular reaction); line (c) is after ozonation (direct molecular reaction and indirect hydroxyl radicals' reaction). González-Vila et al. (2001) cited that four spectral ranges are usually considered, which include a series of prominent peaks: alkyl region (0–50 ppm; methyl groups: around 20 ppm, saturated alkane chains: around 30 ppm, branched aliphatics: around 40 ppm); overlap region (50–60 ppm; methoxy groups: 56 ppm); O-alkyl region (60–100 ppm; carbohydrate-derived: 71 ppm); aromatic:unsaturated region (100–160 ppm; C-substituted polyphenolic C: 105 ppm, unsubstituted aromatic C: 115 ppm, C-substituted aromatic C: 128 ppm, heterosubstituted: 150 ppm); carboxyl region (160–190 ppm; carboxyl groups: 171 ppm), and carbonyl region: (ketone:quinones: 195 ppm).

The spectrum of Figure 4.12 is divided into two main regions corresponding to carbon associated with c-substituted polyphenolic carbons and carboxyl/carbonyl carbons. The intense decrease after ozonation shows the strong oxidation degraded ability. It is also shown in Figure 4.13 ^{13}C NMR spectra of HAs extracted from Te-Chi Reservoir raw water. The spectrum is divided into two main regions which correspond to carbon associated with saturated alkanes (20-30 ppm) and carboxyl/carbonyl

carbons (155-175 ppm). In the line (b) (Figure 4.13), the peak has the displacement during 165-190 ppm. It is not clear to define the different site shows the peak. The reference indicates the range 165-190 ppm is carboxyl/carbonyl carbons (González-Vila et al., 2001). Therefore, in Figure 4.13 (a) and (b) the peaks are the same between 165 and 190 ppm which is a provisional assumption. Due to the addition of scavenger (carbonate and bicarbonate), the lines (b) in two figures (Figure 4.12 and 4.13) do not show the significant decrease in 165-190range. The lines (c) in two figures (Figure 4.12 and 4.13) are tending flat compared with the lines (a) and (b) , this is because ozone oxidizes most of the functional groups. The alkyl region (20-30 ppm) also displays significant peaks of the fractions. From the larger to the smaller fractions, the alkyl peaks move from the higher value of polymethylene carbon to the lower chemical shifts, representing methyl carbon. This may indicate a trend of reaction moving from stronger branched to weaker straight chain aliphatic carbon structures meanwhile, the molecular weight also decreases. As the fractions decrease, the percent of c-substituted polyphenolic carbons and carboxyl/carbonyl carbons decreases indicative of ozonation degradation. It is also consistent with degradation of NOMs (Newcombe et al., 1997)

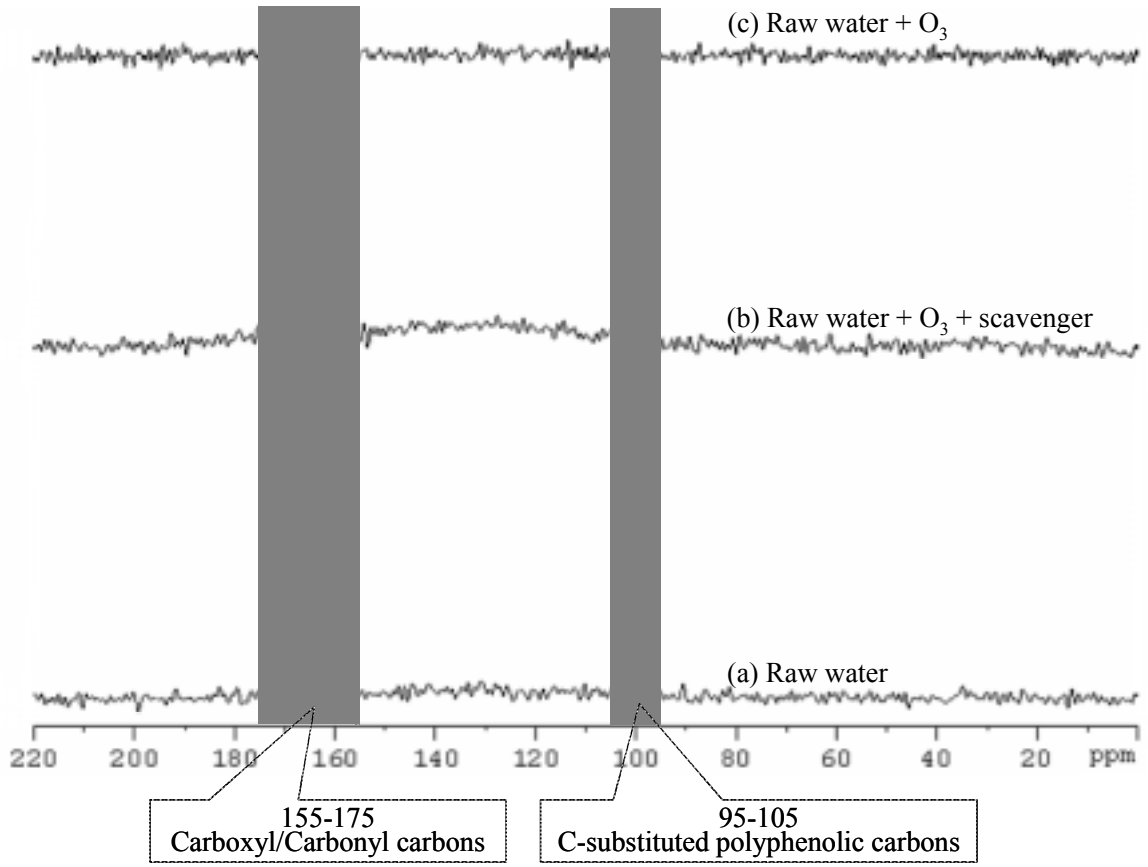

Figure 4.12 ^{13}C NMR spectra of Te-Chi Reservoir raw water (a) before ozonation, (b) after ozonation and scavenger and (c) after ozoantion.

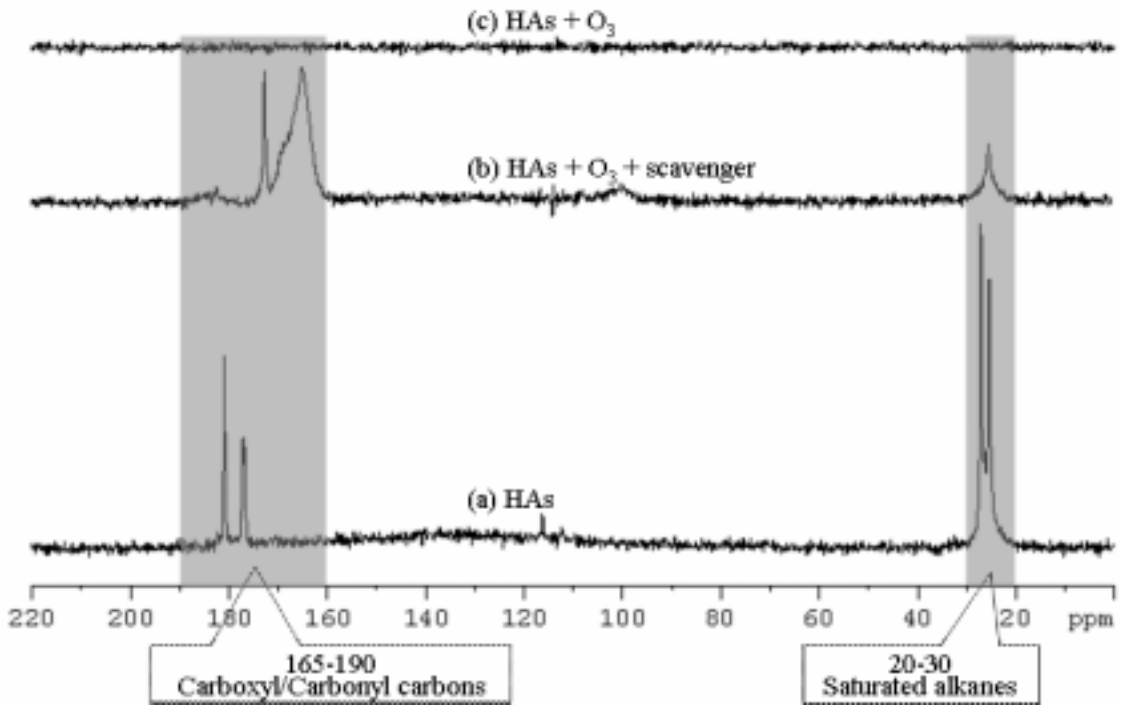

Figure 4.13 ^{13}C NMR spectra of HAs extracted from Te-Chi Reservoir raw water (a) before ozonation, (b) after ozonation and scavenger and (c) after ozoantion.

Chapter 5 Conclusions and suggestions

5.1 Conclusions

1. Due to organic fertilizers were used for a long time, cumulative nitrides and phosphates in water body (red tide) and the drift woods caused by typhoon, the water quality was worse than recent years. The composition of NOMs was separated to five species by XAD-8 resin. There were HAs (24.3%), FAs (7.9%), hydrophobic neutrals (25.2%), hydrophobic bases (2.2%) and hydrophilic fractions (40.4%). The highest DBPFP was HAs which was also the main carcinogenic or mutagenic by-products during disinfection. In this study, the ratios of (THMFP+HAAFP)/(AOXFP) are between 0.1 and 0.95. The highest value was HAs (0.95) which meant it was the carcinogenic DBPs.

2. This study used the oscilloscope to monitor the ORP, DO_3 and pH, and applied UV spectrophotometer (Cary50) to collect the A_{254} values. The measurement of hydroxyl radicals were detected successfully by HPLC with coumarin. These data provide the direct profiles to understand the ozonation mechanism.

3. These data (ORP, DO_3, pH, hydroxyl radicals and A_{254}) could be used to develop an additional Nernst model in ozonation.

4. The spectra of FTIR and ^{13}C NMR indicated the change of functional group after ozonation (direct and indirect reaction) and ozonation with scavenger (direct reaction) obviously. The peaks of carbon in each different functional group were almost decreased completely by ozonation.

5.2 Suggestions

1. Due to the measurement of hydroxyl radicals were successful; the preliminary model was developed in this study. There are many different types of target compounds need to be investigated in the future. Therefore, the complicate compounds of modified Nernst equation for different cases should be investigated.

2. The application of catalyst to enhance the efficiency of ozonation was paid attention by recent researches. The mechanism and catalyst's recovery would be an important investigation.

References

Acero, J. L., Javier, B. F., Francisco, J. R. and Cecilia, M., (2003), "Oxidation of acetamide herbicides in natural waters by ozone and by the combination of ozone/hydrogen peroxide: kinetic study and process modeling", Ind. Eng. Chem. Res., 42(3): 5762-5769.

Alaton, I. A., Kornmuller, A. and Jekel, M. R., (2002), "Ozonation of spent reactive dye-baths: effect of HCO_3^-/CO_3^{2-} alkalinity", J. Environ. Eng., 128(8): 689-696.

APHA, AWWA and WEF (1998). Standard methods for examination of water and wastewater, 20th Edition. American Public Health Association, Washington D.C., USA.

Baban, A., Yediler, A., Lienert, D., Kemerdere, N. and Kettrup, A., (2003), "Ozonation of high strength segregated effluents from a woollen twxtile dyeing and finishing plant", Dyes and Pigments, 58(2): 93-98.

Barrow, G. M., (1988) "Physical Chemistry" McGraw-Hill, NewYork.

Benitez F. J., Jesus, B. H. and Gonzalez, T., (1994), "Degradation by Ozone and UV radiation of the herbicide cyanazine", Ozone: Sci. & Eng., 16: 213-234.

Buxton, G. V., Greenstock, C. L., Helman, W. P. and Ross, A. B., (1988), "Critical review of rate constants for reactions of hydrated electrons, hydrogen atoms and hydroxyl radicals ($\cdot OH/\cdot O^-$) in aqueous solution", J. Phy. and Chem. Ref. Data, 17(2): 513-886.

Calace, N., Capolei, M., Lucchese, M. and Petronio, B. M., (1999), “The structural composition of humic compounds as indicator of organic carbon sources”, Talanta, 49(2): 277–284.

Chien, Y. C., Wang, H. P., Lin, K. S., Huang, Y. J. and Yang, Y. W., (2000), “Fate of bromine in pyrolysis of printed circuit board wastes”, Chemosphere, 40(4): 383-387.

Chu, P. M., Guenther, F. R., Rhoderick, G. C. and Lafferty, W.J., (1999), “The NIST Quantitative Infrared Database”, J. Res. Natl. Inst. Stand. Technol., 104: 59-81.

Chu, W. and Ma, C. W., (2000), “Quantitative prediction of direct and indirect dye ozonation kinetics”, Wat. Res., 34(12): 3153-3160.

Chu, W. and Ching, M. H., (2003), “Modeling the ozonation of 2, 4-dichlorophoxyacetic acid through a kinetic approach”, Wat. Res., 37(1): 39-46.

Dilling, J. and Kaiser, K., (2002), “Estimation of the hydrophobic fraction of dissolved organic matter in water sample using UV photometry”, Wat. Res., 36(20): 5037-5044.

Goel, S., Hozalski, R. M. and Bouwer, E. J., (1995), “Biodegradation of NOM: effect of NOM source and ozone dose”, J. Am. Water Works Assoc., 87(1): 90-105.

González-Vila, F. J., Lankes, U. and Ludemann, H. D., (2001), “Comparison of the information gained bypyrolytic techniques and NMR spectroscopy onthe structural features of aquatic humicsubstances”, Journal of Analytical

and Applied Pyrolysis, 58–59: 349–359.

Hafidi, M., Amir, S. and Revel, J. C., (2005), "Structural characterization of olive mill waster-water after aerobic digestion using elemental analysis, FTIR and ^{13}C NMR", Process Biochemistry, 40(8): 2615–2622.

Hoigné, J. and Bader, H., (1983), "Rate constants of reactions of ozone with organic and inorganic compounds in water. Ⅱ. Dissociatin organic compounds", Wat. Res., 17: 185-194.

Ho, L., Gayle, N. and Croue, J. P., (2002), "Influence of the character ofNOM on the ozonation MIB and geosmin", Wat. Res., 36(3): 511-518.

Hoigné, J., Bader, H., Haag, W. R. and Staehelin, J., (1985), "Rate constants of reactions of ozone with organic and inorganic compounds in water - III. Inorganic compounds and radicals", Wat. Res., 19(8): 993-1004.

Hoigné, J. and Bader, H., (1976), "The role of hydroxyl radical reactions in ozonation processes in aqueous solutions", Wat. Res., 10(5): 377-386.

Kitis, M., Karanfil, T., Wigton, A. and Kilduff, J. E., (2002), "Probing reactivity of dissolved organic matter for disinfection by-product formation using XAD-8 resins adsorption and ultrafiltration fractionation", Wat. Res., 36(15): 3834-3848.

Kleiser, G. and Frimmel, F. H., (2000), "Removal of precursors for disinfection by-products (DBPs) differences between ozone- and OH-radical-induced oxidation", Sci. Total Environ., 256(1): 1-9.

Ko, Y. W., Braun, G. A. and Frimmel, F. H., (2000), "Effect of Preozonation on the Formation of Chlorinated Disinfection By-products for River Ruhr**",**

Acta hydrochim. hydrobiol., 28 (5): 256-261.

Landgraf, S., (2001), “Application of semiconductor light sources for investigations of photochemical reactions”, Spectrochim. Acta Part A, 57(10): 2029–2048.

Leenheer, J. A., (1981), “Comprehensive approach to preparative isolation and fractionation of dissolved organic carbon from natural waters and wastewaters”, Environ. Sci. Technol., 15(5): 578-587.

Leenheer, J. A., Nanny, M. A. and Mclntyre, C., (2003a), “Terpenoids as major precursors of dissolved organic matter in landfill leachates, surface water, and groundwater”, Environ. Sci. Technol., 37(11): 2323-2331.

Leenheer, J. A., Wershaw, R. L., Brown, G. K. and Reddy, M. M., (2003b), “Characterization and diagnosis of strong-acid carboxyl groups in humic substances”, Applied Geochem., 18(3): 471-482.

Louit, G., Foley, S., Cabillic, J., Coffigny, H., Taran, F., Valleix, A., Renault, J. P. and Pin, S., (2005), “The reaction of coumarin with the OH radical revisited: hydroxylation product analysis determined by fluorescence and chromatography”, Radiation Physics and Chemistry, 72(2-3): 119-124.

Ma, C. W. and Chu, W., (2001), “Photodegradation mechanism and rate improvement of chlorinated aromatic dye in non-ionic surfactant solutions”, Wat. Res., 35(10): 2453-2459.

Ma, J. and Graham, N. J. D., (2000), “Degradation of atrazine by manganese-catalyzed ozonation-influence of radical scavengers”, Wat. Res., 34(15): 3822-3828.

Marhaba T. F. and Van, D., (2000), “The variation of mass and disinfection by-product formation potential of dissolved organic matter fraction along a conventional surface water treatment plant”, J. Hazard Mater., A74(3): 133-147.

McGhee, Terence J., (1991), “Water supply and sewerage”, McGRAW-HILL, New YORK.

Nakao, L.S., Ouchi, D. and Augusto, O., (1999), “Oxidation of Acetaldehyde by Peroxynitrite and Hydrogen Peroxide/Iron(II). Production of Acetate, Formate, and Methyl Radicals”, Chem. Res. Toxicol., 12(10): 1010.

Newcombe, G., Drikas, M., Assemf, S. and Beckett, R., (1997), “Influence of characterised natural organic material on activated carbon adsorption I. Characterisation of concentrated Reservoir water”, Wat. Res., 31(5): 965-972.

Nicoli, M. C., Toniolo, R. and Anese, M., (2004), “Relationship between redox potential and chain-breaking activity of model systems and foods”, Food Chemistry, 88: 79-83.

Peña, M., Coca, M., Gonzalez, G., Rioja, R. and Garcia, M.T., (2003), “Chemical oxidation of wastewater from molasses fermentation with ozone”, Chemosphere, 51(9) 893-900.

Pi, Y., Schumacher, J. and Jekel, M., (2005), “Decomposition of aqueous ozone in the presence of aromatic organic solutes”, Wat. Res., 39(1): 83-88.

Pomes, M. L., Larive, C. K., Thurman, E. M., Green, W. R., Orem, W. H., Rostad, C. E., Coplen, T. B., Cutak, B. J. and Dixon, A. M., (2000), “Sources

and haloacetic acid/trihalomethane formation potentials of aquatic humic substances in the Wakarusa river and Clinton Lake near Lawrence, Kansas", Environ. Sci. Technol., 34(20): 4278-4286.

Prado, J., Arantegui, J., Chamarro, E. and Esplugas, S., (1994), "Degradation of 2, 4–D by ozone and light", Ozone: Sci. & Eng., 16(3): 235-245.

Rice, R. G., Robson C. M., Miller G. W. and Hill A. G. M., (1981), "Use of ozone-bromide reactions", J. Am. Water Works Assoc., 85(1):63-72.

Rook, J. J., (1977), "Chlorination reactions of fulvic acids in natural waters", Environ. Sci. Technol., 11(5): 478-482.

Saito, H. and Hyodo, T., (2003), "Improvement in the gamma-ray timing measurements using a fast digital oscilloscope", Radiation Phy. Chem., 68(3-4): 431-434.

Sarma, L., Devasagayam, T. P., Mohan, H., Mittal, J. P. and Kesavan, P. C., (1996), "Mechanisms of protection by buthionine sulphoximine against γ-ray-induced micronuclei in polychromatic erythrovcytes of mouse bone marrow", Int. J Radiat. Biol., 69(5): 633-643.

Staehelin, J. and Hoigné, J., (1985), "Decomposition of ozone in water in the presence of organic solutes acting as promoters and inhibitors of radical chain reactions", Environ. Sci. Technol., 19(12): 1206-13.

Staehelin, J. and Hoigné, J., (1982), "Decomposition of ozone in water—rate of initiation by hydroxide ions and hydrogen peroxide", Environ. Sci. Technol., 16(10): 676-681.

Thurman, E. M. and Malcolm, R. L., (1981), "Preparative isolation of

aquatic humic substances", Environ. Sci. Technol., 15(4): 463-466.

Utsumi, H., Han, Y. H. and Ichikawa, K., (2003), "A kinetic studt of 3-chlorophenol enhanced hydroxyl radical generation during ozonation", Wat. Res., 37(20): 4924-4928.

Von Gunten, U., (2003a), "Ozonation of drinking water: Part I. Oxidation kinetics and product formation", Wat. Res., 37(7):1443-1467.

Von Gunten, U., (2003b), "Ozonation of drinking water: Part II. Disinfection and by-product formation in presence of bromide, iodide or chlorine", Wat. Res., 37(7): 1469-1487.

White, D. M., Garland, D., Jasprit, S. N. and Woolard, C. R., (2003), "Natural organic matter and DBP formation potential in Alaskan water supplies", Wat. Res., 37(4): 939-947.

Wang, X., Huang, X., Zuo, C. and Hu, H., (2004), "Kinetics of quinoline degradation by O3/UV in aqueous phase", Chemosphere, 55(5): 733-741.

Zuo, Y., (2003), "Light-induced formation of hydroxyl radicals in fog waters determined by an authentic fog constituent, hydroxymethanesulfonate", Chemosphere, 51(3): 175-179.

張裕和, (1997), "水源中各類有機物不同分子量分佈對生成消毒副產物的影響及其控制策略之探討", 東海大學環境科學研究所碩士論文.

李福順, (1998), "大甲溪流域及旗下游豐原淨水廠水體中有機性消毒副產物前驅物質分佈特性之研究", 東海大學環境科學研究所碩士論文.

辛汎峰, (1999), "以臭氧及膜濾法降低優氧化水體中同有機成分生成消

毒副產物潛能之探討”，東海大學環境科學系碩士班碩士論文.

吳家興, (2000), “台灣地區水庫水源特性分及消毒副產物生成潛能之探討”，東海大學環境科學碩士班碩士論文.

陳峙霖, (2001), “以預臭氧對腐植酸生成消毒副產物特性之探討”，東海大學環境科學研究所碩士論文.

蔡美純, (2002), “從水中天然有機物官能基變化探討前臭氧/粒狀活性碳反應機制”，東海大學環境科學研究所碩士論文.

宋曉帆, (2003), “利用高級處理程序及高速擷取設備輔助監測水體中天然有機物官能基特性變化及降低消毒副產物生成潛能探討”，東海大學環境科學研究所碩士論文.

梁永瑩, (2004), “Applying Oscilloscope to Investigate the Direct and Indirect Ozone Reactions”，東海大學環境科學研究所碩士論文.